SALAM-MED
Sustainable Approaches to Land and water Management in Mediterranean Drylands

Deliverable D2.3

Report on improved water harvesting approaches

Delivery Date: 24/10/2025

Dissemination Level: Public

Status: Final version

Keywords: Water Harvesting, wadi terraces, Subsurface Water Retention Technologies (SWRT), Managed Aquifer Recharge (MAR), Soil and Water Conservation

This project has received funding from the Partnership on Research and Innovation in the Mediterranean Area joint program (PRIMA) under grant agreement No 2123.

Disclaimer

Outline

This document presents the results of Task 2.3 of SALAM-MED project, "Practical solutions to restore degraded lands". The task developed a series of experiments in three of the project's Living Labs, targeting selected technologies for restoring degraded landscapes through water harvesting. The technologies considered were:

Subsurface Water Retention Technology (SWRT) for argan forest restoration in the Moroccan Living Lab

Managed Aquifer Recharge in the Tunisian Living Lab

Levelled terraces for water harvesting in the "Wadis" in the Egyptian Living Lab

Document Information

Project Title: Sustainable Approaches to Land and Water Management in Mediterranean Drylands

Grant Agreement: 2123

Project Acronym: SALAM-MED

Project Funder: Partnership on Research and Innovation in the Mediterranean Area joint program (PRIMA).

Related work package: WP2

Lead Beneficiary: University of Florence

Submission date: 27/10/2025

Nature: Report

Dissemination Level: Public

Version: Final

Authors:

Giulio Castelli*, University of Florence

Mohamed Ait-El-Mokhtar, Hassan II University, Casablanca, Morocco

Mongi Ben Zaied, Institut des Régions Arides

Ahmed Elshenawy, Desert Research Center

* Correspondence: giulio.castelli@unifi.it

Executive Summary

This document presents the results of Task 2.3 of SALAM-MED project, “Practical solutions to restore degraded lands”. The task developed a series of experiments in three of the projects’ Living Labs, targeting selected technologies for restoring degraded landscapes through water harvesting.

The technologies considered were:

Subsurface Water Retention Technology (SWRT) for argan forest restoration in the Moroccan Living Lab

Managed Aquifer Recharge in the Tunisian Living Lab

Levelled terraces for water harvesting in the “Wadis” in the Egyptian Living Lab

The structure of the deliverable comprises 3 sections, each of these organized with an introduction, a materials and methods section, a results section, a discussion and a conclusion. Implication for policymakers are provided for each technology.

List of Figures

List of Tables

List of Acronyms and Definitions

Arbuscular Mycorrhizal Fungi: AMF

Electrical resistivity measurement devices: ERT

Managed Aquifer Recharge: MAR

Subsurface Water Retention Technology: SWRT

List of Beneficiaries

Desertification Research Center, University of Sassari	NRD	Italy
Università degli studi di Firenze	UNIFI	Italy
CNR, Inst. for Sustainable Plant Protection	CNR-IPSP	Italy
Centre Int. Hautes Etudes Agronomiques Méditerranéennes	CIHEAM	France
Desert Research Center	DRC	Egypt
Institut des Régions Arides	IRA	Tunisia
Cadi Ayyad University - Faculté des Sciences Semlalia	UCA	Morocco
Médenine Agro Tech	MAT	Tunisia

Table of Contents

1. Moroccan Living Lab "TAGANT"

1.1. Introduction and statement of the research gaps

Argania spinosa L. Skeels is a tree species native to Morocco and holds significant importance in the national flora. It is the second most prevalent species by coverage, spanning an estimated 950,000 hectares (Chakhchar et al., 2022; Lefhaili, 2010). The tree is valued for its fruit, which produces oil used in culinary, cosmetic, and medicinal applications (Lefhaili, 2010). The argan ecosystem faces increasing degradation due to climate change, overgrazing, illegal firewood harvesting, and deforestation. These pressures have reduced forest density from 100 trees per hectare to less than 30 over the last century (Chakhchar et al., 2022).

Reforestation efforts have struggled due to the arid conditions of southwest Morocco, where water scarcity limits the establishment of seedlings, leading to low success rates for reforestation (Defaa et al., 2015; Ghazali et al., 2021). Hence, there is a pressing need to find alternatives to promote reforestation success, such as water harvesting technologies. Subsurface Water Retention Technology (SWRT) involves installing impermeable, biodegradable membranes below the root zone to conserve water and nutrients. This technique has proven effective in highly permeable soils, enhancing plant water retention, nutrient absorption, and drought resilience, which is critical for argan seedlings in arid regions (Guber et al., 2015).

Arbuscular Mycorrhizal Fungi (AMF) are beneficial soil microorganisms that form symbiotic relationships with about 78% of vascular plants, enhancing nutrient and water absorption, particularly in drought conditions (Begum et al., 2019). Research shows that AMF can support plant growth (Bahadur et al., 2019), nutrient accumulation, and water status, making plants more resilient to environmental stress (Kapoor et al., 2013). These fungi boost plants' ability to withstand drought by improving root water uptake, optimizing stomatal function, and supporting essential biochemical processes (Tang et al., 2022).

This is the first study to evaluate the application of SWRT and AMF on *Argania spinosa* reforestation. It investigates their individual and combined effects on soil moisture, growth, physiology, and biochemistry of argan seedlings planted in Morocco's Essaouira region. By identifying effective and sustainable practices, this research aims to inform reforestation strategies that can help preserve and restore the unique argan ecosystem, which is vital to the livelihoods of local communities and the regional environment.

1.2. Materials and methods

1.2.1. Study Area

The field experiment took place in Id Bouzid, Morocco (31°19'29.3"N, 9°32'32.8"W), in a semi-arid climate at 360 m altitude. Conducted over a 2.7-hectare organic farm without herbicides or chemical fertilizers, the experiment followed uniform tillage and manual weed removal. Soil characteristics included 34.58% sand, 48.51% silt, and 16.84% clay, with a pH of 7.39 and electrical conductivity (EC) of 0.282 mS cm^{-1}.

1.2.2. Experimental design

The study used one and two-year-old argan seedlings from the Essaouira ecotype and applied four treatments: (1) Control (Ct), (2) SWRT (using biodegradable plastic buried under each plant), (3) AMF inoculation (M), and (4) a combined SWRT+AMF treatment (M+SWRT). Each treatment had 25 replicates, totaling 100 plants in a randomized design. AMF were native to the argan forest, multiplied using maize, and then applied as a 30 g inoculum in each plant's rhizosphere. Non-inoculated plants

received sterilized inoculum. Transplanting was performed in February 2023, and seedlings were irrigated once each month with 50 liters.

1.2.3. Soil measurements and volumetric water content

One year after transplanting, soil samples were collected near the roots for physicochemical analysis. The soil was air-dried for 48 hours before testing. To measure pH and EC, 5 g of 2 mm sieved soil was mixed with 25 mL of distilled water (1:5 v/v ratio), agitated for 30 minutes, and measured using a pH meter and a conductivity meter.

Total organic carbon (TOC) and organic matter (OM) were determined using the Aubert method (Aubert, 1978). Total organic carbon expressed as a percentage of dry matter is given by the following formula:

$$\%\,TOC = \frac{(Vc - Vs)x\ F}{PxVc}$$

Available phosphorus (AP) was measured using the colorimetric method by (Olsen & Sommers, 1982). The absorbance was read at 820 nm using a spectrophotometer. Soil volumetric water content was measured monthly with a PR2 Profile Probe (Delta-T Devices, Cambridge, UK) at depths of 10, 20, 30, and 40 cm.

1.2.4. Physiological measurements

Physiological measurements were taken on fully developed leaves. Chlorophyll fluorescence (Fv/Fm), indicating PSII efficiency, was measured using a fluorometer (Opti-sciences OSI 30p) after 20 minutes of dark adaptation (five readings per treatment) (Baker, 2008). Stomatal conductance (gs) was recorded using a portable porometer (Leaf Porometer LP1989) on the lower leaf surface between 9:00 and 11:00 a.m. on sunny days.

Photosynthetic pigments were extracted following Arnon's method (Arnon, 1949). An amount of 50 mg of crushed leaf tissue was homogenized in 4 mL of 80% acetone, then centrifuged for 10 minutes at 10,000 × g. Absorbance was measured at 663, 645, and 480 nm for chlorophyll a, chlorophyll b, and carotenoids, respectively, using a spectrophotometer (UV-3100PC). Concentrations were calculated based on standard equations.

$$Chlorophyll\ a\ \left(\frac{mg}{g}\right) = [(12.7 \times OD663) - (2.69 \times OD645)] \times \frac{V}{1000} \times FW$$

$$Chlorophyll\ b\ \left(\frac{mg}{g}\right) = [(22.9 \times \mathrm{OD645}) - (4.68 \times \mathrm{OD663})] \times \frac{V}{1000} \times \mathrm{FW}$$

$$Total\ Chlorophyll\ \left(\frac{mg}{g}\right) = [OD480 + (0.114 \times OD663) - (0.638 \times OD645)] \times \frac{V}{1000} \times FW$$

Where, V = final volume of the extract, and FW = fresh weight.

1.2.5. Biochemical leaf traits measurement

Total soluble sugars were measured in fully expanded argan leaves using the (Dubois et al., 1956) method. The absorbance was read at 485 nm using a spectrophotometer. For total soluble proteins and antioxidant enzymes, 0.1 g of leaf samples were ground in phosphate buffer with PVPP and EDTA, then centrifuged at 18,000 × g. Protein content was quantified using the protocol of (Bradford, 1976). PPO activity was measured following the method of (Gauillard et al., 1993) using catechol oxidation

monitoring at 410 nm. The solution used included enzyme extract (0.1 mL), catechol (50 mM), and K2HPO4/KH2PO4 buffer (100 mM, pH 6). POX activity was evaluated according to Tejera García et al. method (Tejera García et al., 2004). PPO and POX enzyme activities were expressed in unit mg protein^{-1}.

Malonyldialdehyde (MDA) levels, indicating lipid peroxidation, were measured according to the protocol of (Savicka & Škute, 2010) the absorbance was read at 450, 532, and 600 nm. Hydrogen peroxide (H_2O_2) concentration was determined using the method of (Velikova et al., 2000) by mixing leaf extracts with potassium iodate, reading absorbance at 390 nm after one-hour dark incubation.

1.2.6. Statistical analysis

Data are presented as mean values ± standard error (S.E.), based on five replicates for soil moisture and argan growth/physiological traits, and three replicates for biochemical analyses. Statistical analysis was performed using analysis of variance (ANOVA) in SPSS version 25.0 (IBM, Armonk, NY, USA). Tukey's test was applied at a significance level of *p* ≤ 0.05 to compare mean values across treatments.

1.3. Results

1.3.1. Soil Physicochemical Properties

The results showed that soil pH varied across treatments, with values ranging from 7.89 to 8.10, the highest in M and M+SWRT treatments and the lowest in the control (Ct) (Table 1). Mycorrhiza alone or with SWRT significantly increased electrical conductivity (EC) by 31% and 43%, respectively, compared to the control. Available phosphorus (AP) levels also rose significantly in all treatments, with the highest increase of 50% in the M+SWRT group.

Total nitrogen (NTK) levels were significantly higher in all treatments, with an 80% increase in M+SWRT, followed by 69% in SWRT and 54% in M alone. Total organic carbon (TOC) increased by 26% and 51% in M and M+SWRT treatments, respectively, while SWRT showed a modest 8% rise. Similarly, organic matter (OM) levels were enhanced by 27% in M and 51% in M+SWRT, while SWRT led to a modest 7% increase.

Table 1. Soil physicochemical characteristics before and after one year of argan seedling transplantation.

	pH	EC (µS cm−1)	AP (ppm)	NTK (g Kg−1)	TOC (%)	OM (%)
Ct	7.89 ± 0.06b	237.33 ± 6.02c	31.46 ± 0.30b	3.06 ± 0.32c	0.39 ± 0.03c	0.67 ± 0.05c
SWRT	7.99 ± 0.06ab	205.66 ± 5.03d	40.60 ± 2.27a	5.17 ± 0.03a	0.42 ± 0.00c	0.72 ± 0.00c
M	8.10 ± 0.02a	312.00 ± 4.58b	43.40 ± 4.34a	4.72 ± 0.06b	0.49 ± 0.02b	0.85 ± 0.03b
M+SWRT	8.07 ± 0.01a	340.66 ± 8.50a	47.06 ± 2.11a	5.51 ± 0.08a	0.59 ± 0.03a	1.01 ± 0.05a

Ct: control; SWRT: subsurface water retention technology; M: mycorrhiza; M+SWRT: mycorrhiza+ subsurface water retention technology; EC: electrical conductivity; AP: available phosphorus; NTK: nitrogen total Kjeldahl; TOC: total organic carbon; OM: organic matter. Data denoted are means of three replicates (n = 3) ± standard error (SE). Different letters within the same column denote significant differences at p < 0.05 based on Tukey's test.

1.3.2. Soil Moisture Profile

The SWRT treatment consistently showed the highest soil moisture levels across all depths and throughout the two-year study period compared to the control (Figure 1). The most substantial increase was observed at 40 cm depth in December 2023, with a 640% rise relative to the control, while the smallest increase (9%) occurred at 20 cm depth in the same month.

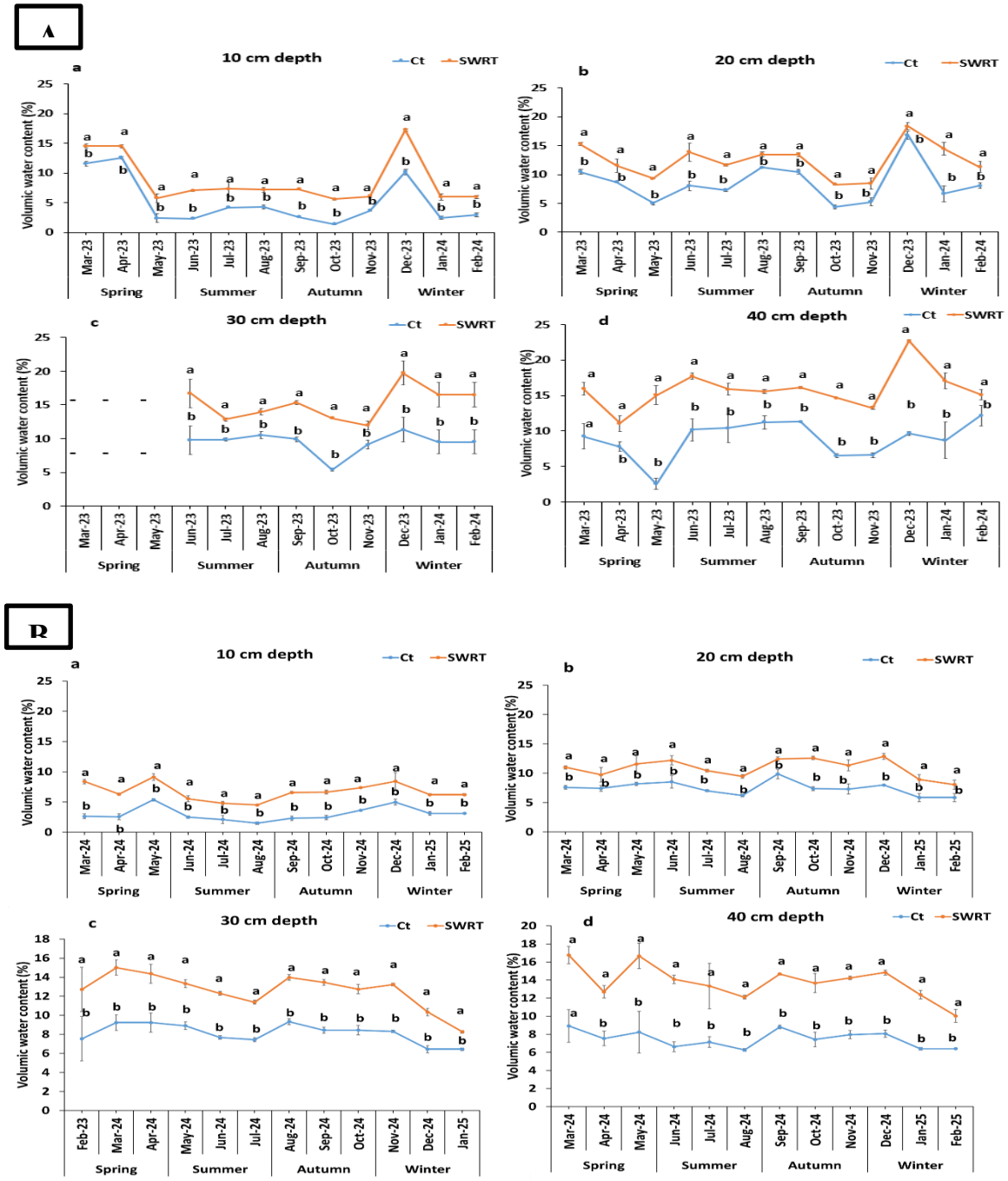

Figure 1. Monthly variation of soil moisture profile in the absence or the presence of subsurface water retention technology treatment at different soil depths in the first (A) and second (B) year after transplantation: (a) 10 cm depth, (b) 20 cm depth, (c) 30 cm depth, (d) 40 cm depth. Ct: control, SWRT: subsurface water retention technology. Data denoted are means of five replicates (n = 5) ± standard error (SE). Different letters within the same month designate significant differences at $p < 0.05$ based on Tukey's test.

1.3.3. Shoot Elongation

Shoot elongation was significantly higher in SWRT, M, and M+SWRT treatments compared to the control. While no differences were observed between treatments immediately after transplanting (March and April 2023), SWRT and M+SWRT treatments showed marked increases over the following months, reaching 168% and 208% improvement, respectively, compared to the control by February

2024 (Figure 2A). The effect persisted throughout the following year. By February 2025, increases of 154.25% and 172.72% were recorded for SWRT and M+SWRT, respectively, compared to the control (Figure 2B).

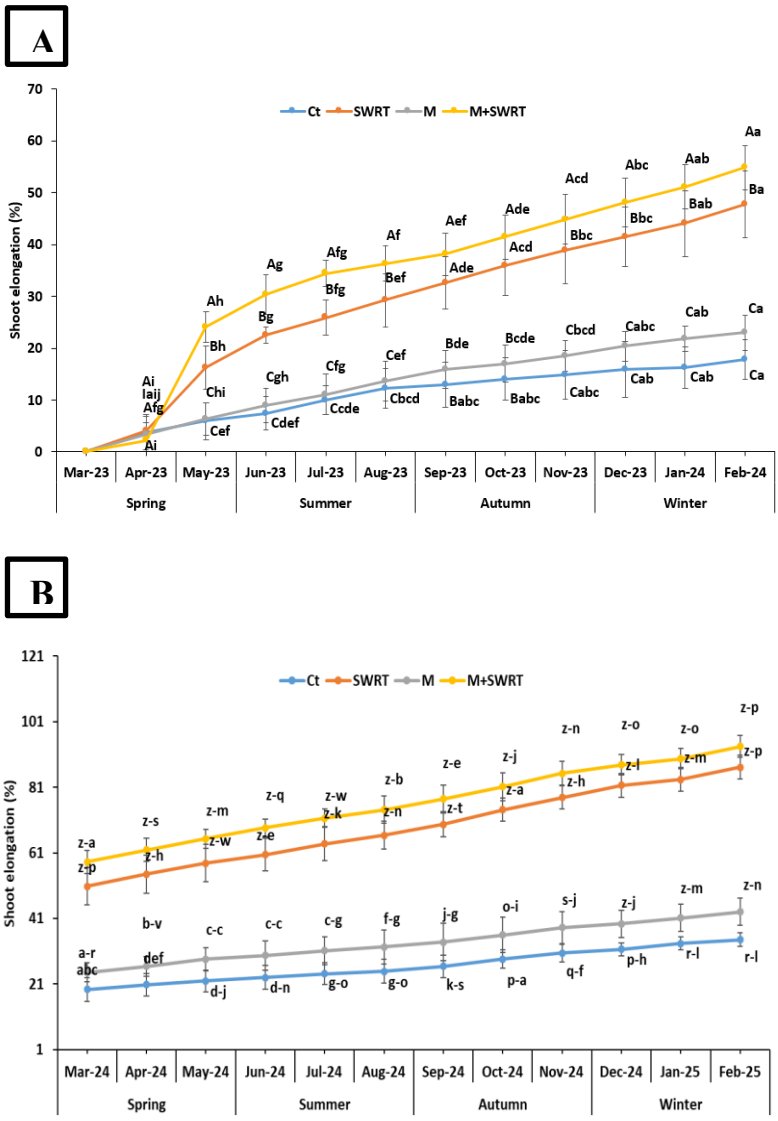

Figure 2. Monthly variation of shoot elongation of argan seedlings under different treatments in the first (A) and second year (B) post-transplantation: control (Ct), subsurface water retention technology (SWRT), mycorrhiza (M), and the combined treatment (M+SWRT). Data denoted are means of five replicates (n = 5) ± standard error (SE). Data represent mean values from five replicates (n = 5) ± standard error (SE). Capital letters within each month indicate significant differences between treatments, while lower-case letters within each treatment represent significant differences across months ($p < 0.05$, Tukey's test).

1.3.4. Physiological parameters

The application of SWRT alone and combined with mycorrhiza (M+SWRT) significantly boosted Fv/Fm throughout the two-year study period, compared to the control (Ct), with increases between 4 and 22% (Figure 3A). The largest increases for SWRT (19%, 20%, and 22%) were in July, October, and November 2023, with M+SWRT showing similar peaks (19%, 21%, and 21%) in the same months. In the second year of study, the highest values were observed in April 2024 for both SWRT (11.42%) and

M+SWRT (14.42%), compared to the control (Figure 3B). The M treatment alone showed modest improvements, with increases of 1–8% over Ct (Figure 3).

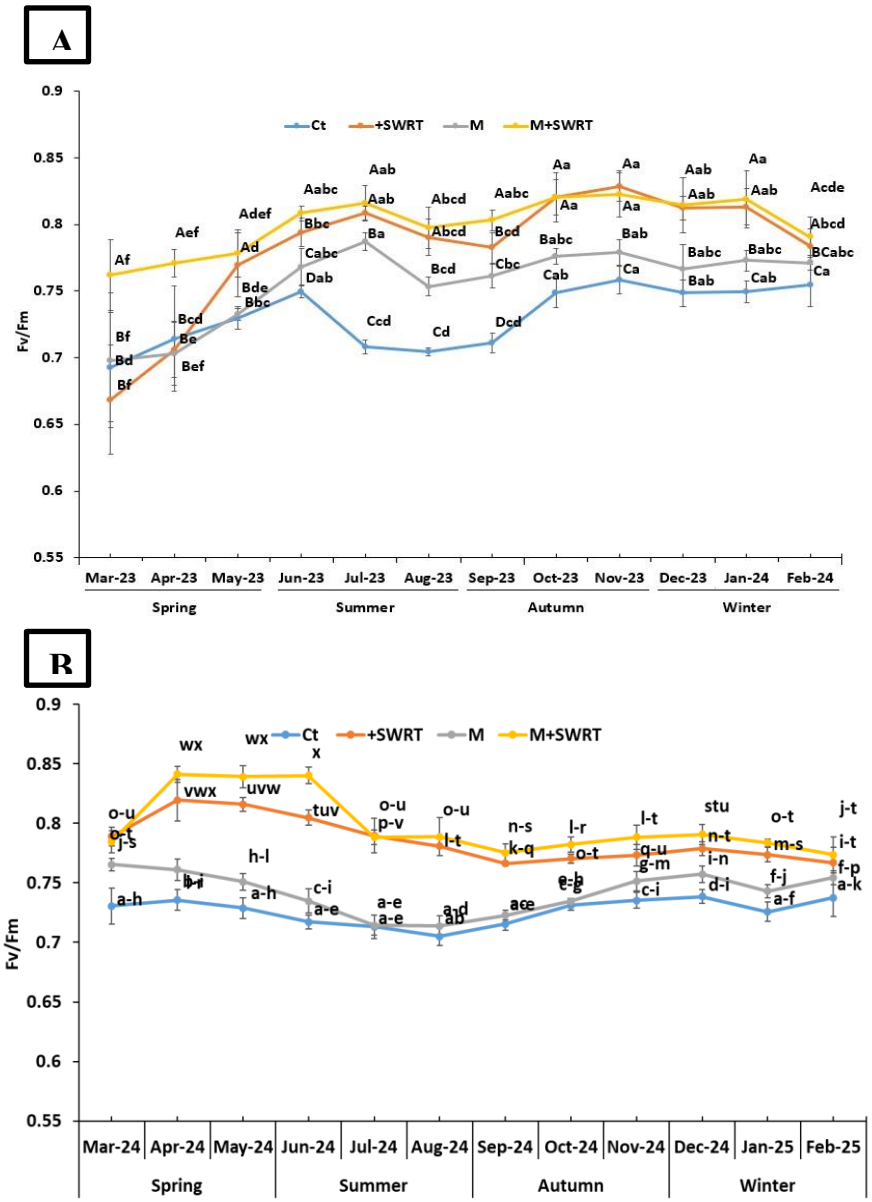

*Figure 3. Monthly variation of chlorophyll fluorescence (Fv/Fm) of argan seedlings under different treatments in the first **(A)** and second **(B)** year post-transplantation: control (Ct), subsurface water retention technology (SWRT), mycorrhiza (M), and the combined treatment (M+SWRT). Data denoted are means of five replicates (n = 5) ± standard error (SE). Data represent mean values from five replicates (n = 5) ± standard error (SE). Capital letters within each month indicate significant differences between treatments, while lower-case letters within each treatment represent significant differences across months ($p < 0.05$, Tukey's test).*

Stomatal conductance (gs) also varied significantly across treatments. M+SWRT consistently recorded the highest gs values, with increases from 18% to 59% compared to the control, peaking in February 2024 (Figure 4A). SWRT followed with a steady increase, showing a maximum 33% improvement in July 2023. The M treatment had moderate gains over Ct, with increases of 11–21%, demonstrating some benefit but less than the combined M+SWRT or SWRT treatments alone. In the second year of

this study, the M treatment showed an improvement, with the highest increase recorded in May 2024 (41.49%); however, it remained less effective than M+SWRT and SWRT (Figure 4B).

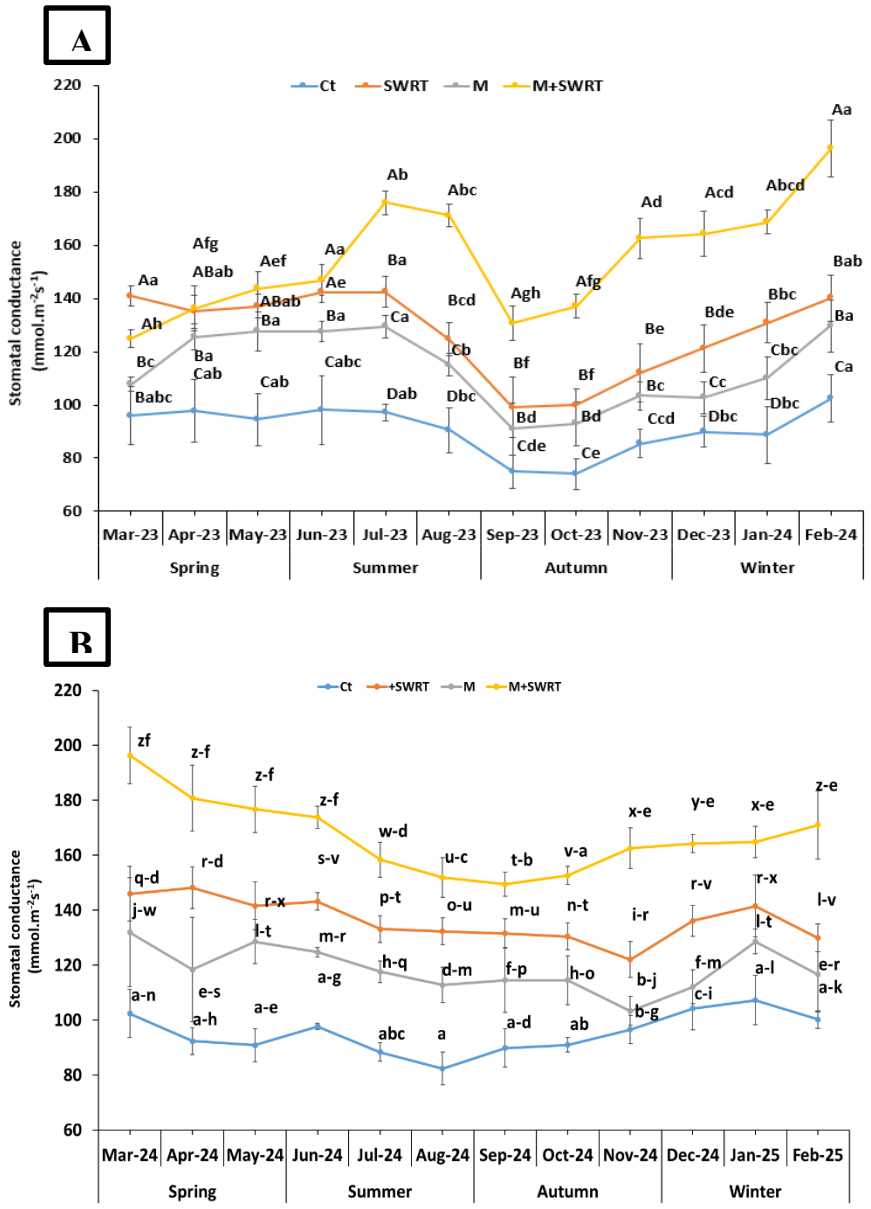

*Figure 4. Monthly variation of stomatal conductance (gs) of argan seedlings under different treatments in the first **(A)** and second **(B)** year post-transplantation: control (Ct), subsurface water retention technology (SWRT), mycorrhiza (M), and the combined treatment (M+SWRT). Data denoted are means of five replicates (n = 5) ± standard error (SE). Data represent mean values from five replicates (n = 5) ± standard error (SE). Capital letters within each month indicate significant differences between treatments, while lower-case letters within each treatment represent significant differences across months ($p < 0.05$, Tukey's test).*

Findings of photosynthetic pigments indicate that both SWRT and mycorrhiza treatments significantly enhanced chlorophyll and carotenoid levels compared to the control (Figure 5). SWRT-treated plants showed the highest increase in chlorophyll a (71%), while the combined M+SWRT treatment had the largest increase in chlorophyll b (64%). For total chlorophyll, M+SWRT and SWRT treatments resulted

in 67% and 68% increases, respectively. Carotenoid levels were highest in the M+SWRT treatment, with a 67% increase, followed by mycorrhiza (38%) and SWRT (22%).

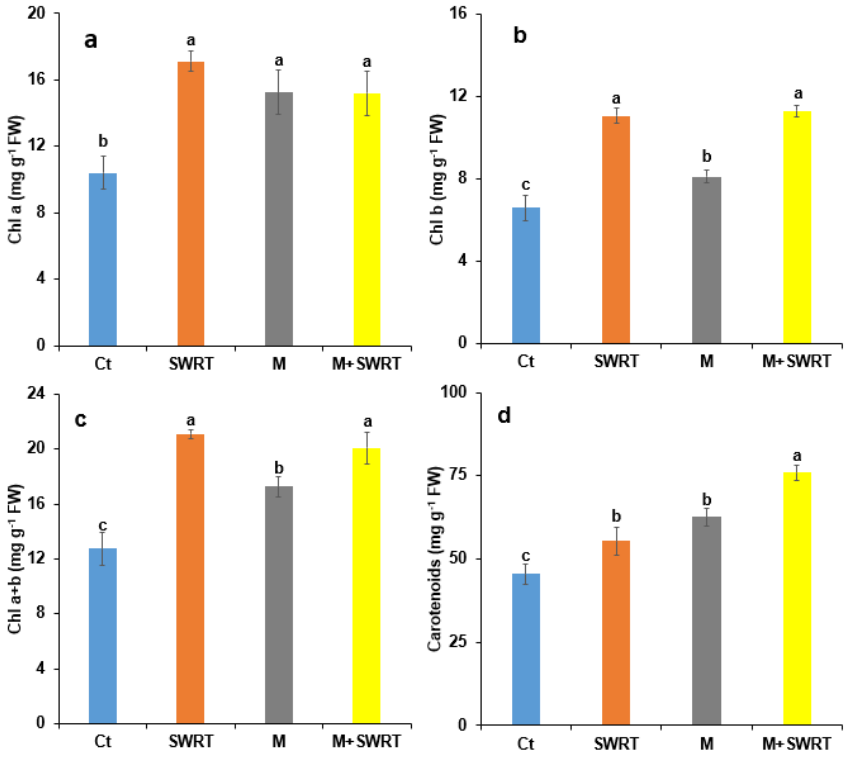

*Figure 5. Effect of subsurface water retention technology and/or mycorrhiza treatments on argan seedlings' photosynthetic pigments content (Chl a (**a**), Chl b (**b**), Chl a+b (**c**) and carotenoids (**d**)). Chl a: chlorophyll a; Chl b: chlorophyll b; Ch a+b: Total chlorophyll; Ct: control, SWRT: subsurface water retention technology, M: mycorrhiza, M+SWRT: mycorrhiza+subsurface water retention technology. Data denoted are means of three replicates (n = 3) ± standard error (SE). Different letters denote significant differences at p < 0.05 based on Tukey's test.*

1.3.5. Stress Markers, Organic Osmolytes Content and Activity of Antioxidant Enzymes

Malondialdehyde (MDA) levels differed significantly across treatments, with M+SWRT-treated plants showing the greatest reduction (33%), followed by SWRT (20%) and mycorrhiza (M) alone (10%) compared to the control (Ct) (Figure 6a). Regarding hydrogen peroxide (H_2O_2) content, M+SWRT demonstrated a notable 14% reduction relative to the control, while mycorrhiza alone reduced H_2O_2 by 20%. The SWRT treatment, however, showed no significant difference in H_2O_2 levels compared to the control (Figure 6b).

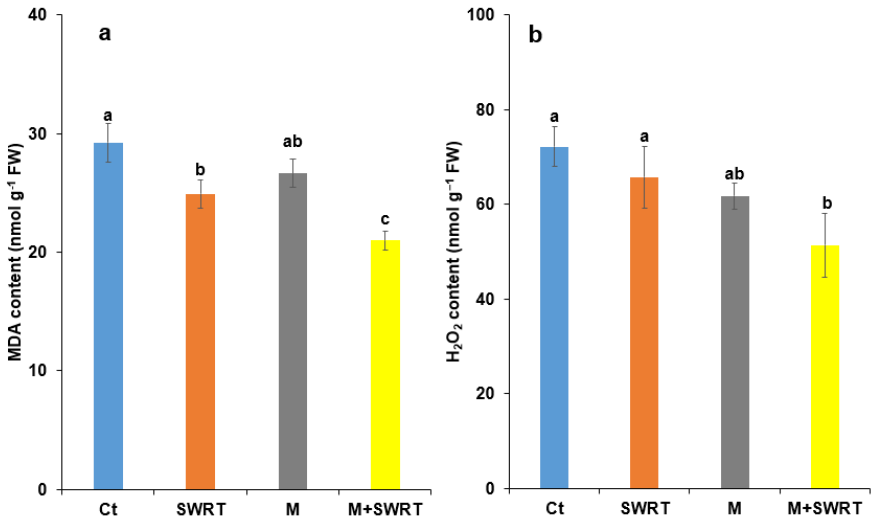

Figure 6. Effects of subsurface water retention technology and/or mycorrhiza treatments on argan seedlings' (a) malondialdehyde and (b) H2O2 accumulations. Ct: control, SWRT: subsurface water retention technology, M: mycorrhiza, M+SWRT: mycorrhiza+subsurface water retention technology, MDA: malondialdehyde. Data denoted are means of three replicates (n = 3) ± standard error (SE). Different letters denote significant differences at p < 0.05 based on Tukey's test.

Figure 7 shows that protein and sugar levels varied significantly among treatments. The M+SWRT treatment produced the highest protein content, with a 36% increase over the control, while SWRT alone showed a moderate increase of 18%. Soluble sugars also peaked with M+SWRT, showing a 57% enhancement, whereas mycorrhiza (M) alone resulted in the lowest increase at 22% compared to the control.

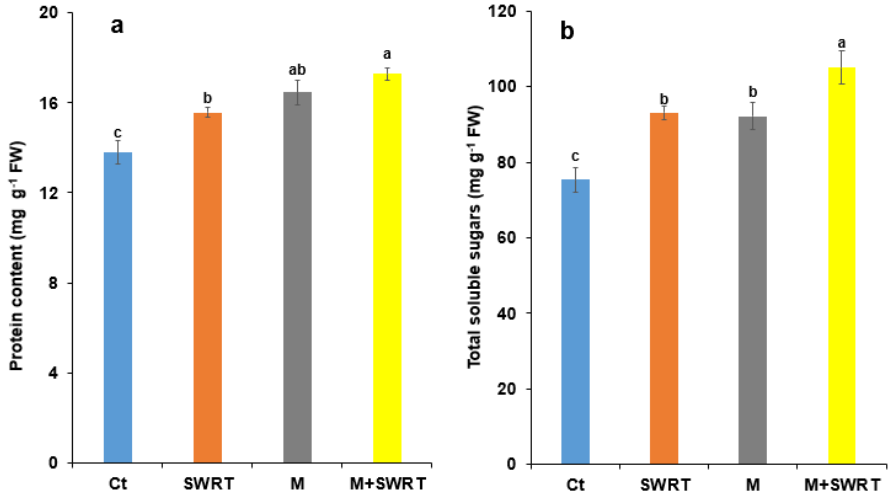

Figure 7. Effects of subsurface water retention technology and/or mycorrhiza treatments on argan seedlings' (a) proteins and (b) total soluble sugars contents. Ct: control; SWRT: subsurface water retention technology; M: mycorrhiza; M+SWRT: mycorrhiza+subsurface water retention technology. Data denoted are means of three replicates (n = 3) ± standard error (SE). Different letters denote significant differences at p < 0.05 based on Tukey's test.

Results indicate significant differences in polyphenol oxidase (PPO) and peroxidase (POX) activities across treatments (Figure 8). The combined M+SWRT treatment led to substantial increases in both PPO and POX activities, with enhancements of 129% and 70%, respectively, over the control. In contrast, SWRT and mycorrhiza (M) applied individually did not show significant increases in either enzyme activity compared to the control.

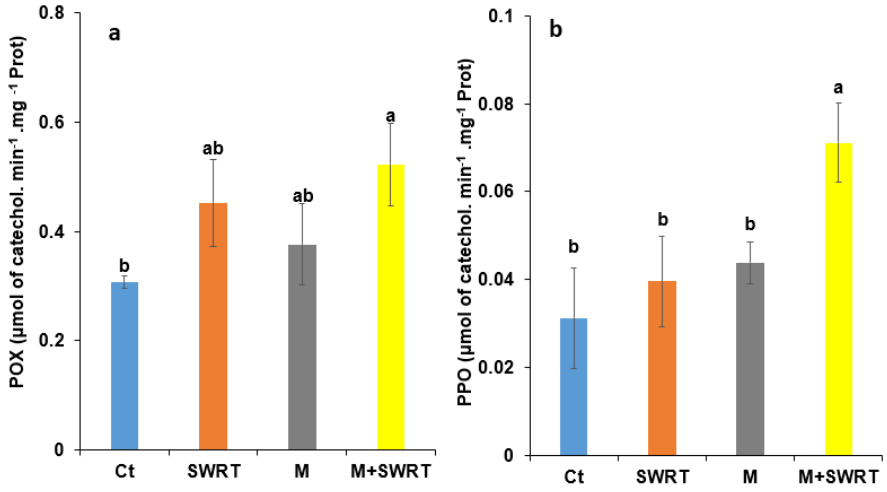

Figure 8. Effects of subsurface water retention technology and/or mycorrhiza treatments on argan seedlings' (a) peroxidase and (b) polyphenol oxidase activities. Ct: control; SWRT: subsurface water retention technology; M: mycorrhiza; M+SWRT: mycorrhiza+subsurface water retention technology; PPO: polyphenol oxidase; POX: peroxidase. Data denoted are means of three replicates (n = 3) ± standard error (SE). Different letters denote significant differences at p < 0.05 based on Tukey's test.

1.4. Discussion

Drought and desertification pose serious threats to ecosystem sustainability, especially in arid and semi-arid regions, which are among the most vulnerable (Zarei, 2018). In Mediterranean areas, the limited reforestation potential is largely due to low rainfall, high evaporation rates, and extensive soil degradation (Luján Soto et al., 2021; Zarei, 2018). These soils are often characterized by low water retention capacity, reduced microbiological biodiversity, and insufficient levels of nutrients and organic matter (León-Sánchez et al., 2020). Therefore, identifying cost-effective methods to enhance drought resilience and improve soil quality is critical to successful reforestation in these degraded landscapes. This study is pioneering in its field-based investigation of the effects of SWRT combined with AMF on argan seedlings, specifically assessing their combined influence on soil quality and plant growth, physiology, and biochemistry.

Our results indicate that applying native AMF, alone or with SWRT, positively impacts soil mineral nutrient levels and pH. The observed increase in soil pH under SWRT is likely attributable to improved soil structure and heightened biological activity, corroborating findings from previous research (Belayneh et al., 2019; León-Sánchez et al., 2020). In contrast, the M and M+SWRT treatments increased soil electrical conductivity (EC), potentially indicating salt accumulation due to limited leaching under these conditions (Lahbouki et al., 2022). These outcomes align with Belayneh et al. (2019), who noted similar changes in soil properties following soil conservation interventions. Available phosphorus (AP) levels rose significantly under M and M+SWRT treatments, a likely result of enhanced phosphorus uptake facilitated by AMF. AMF improve nutrient availability, particularly phosphorus, even under high-pH conditions, by establishing extensive mycelial networks that boost

phosphorus absorption in the rhizosphere, providing plants access to otherwise inaccessible forms of phosphorus (Figueiredo et al., 2021). Moreover, certain mycorrhizal species release organic acids that acidify the rhizosphere locally, further promoting phosphorus solubilization and uptake (Andrino et al., 2021). AMF also produce phosphatase enzymes that release phosphorus from organic matter in the soil (Liu et al., 2021) and can interact with calcium ions, preventing the formation of insoluble calcium phosphate and thus enhancing phosphorus availability (Wahid et al., 2020). This mechanism is further supported by Lahbouki et al. (2022), who showed that SWRT significantly enhances soil phosphorus levels.

The increase in soil total nitrogen observed across treatments may stem from enhanced organic matter content and microbial activity, which bolster nitrogen mineralization rates. These findings are in line with earlier studies (Belayneh et al., 2019; Lahbouki et al., 2022), which recorded similar total nitrogen increases following SWRT and/or AMF applications. Organic matter content, particularly under the M+SWRT treatment, showed a marked improvement, suggesting that combining SWRT with AMF significantly boosts soil nutrient and water retention capacities, a finding consistent with other studies (Belayneh et al., 2019; Lahbouki et al., 2022). Soil moisture results highlight that SWRT's application notably improved water content at various depths, with the most significant enhancement observed at 40 cm depth. This treatment had a pronounced positive effect on the soil's water-holding capacity throughout the year. Aoda et al. (2021) observed similar outcomes, reporting that SWRT application, through biodegradable plastic, enhances water retention in the root zone (at 15 and 30 cm depths) and minimizes water leaching, leading to more efficient water use within the soil profile. The results suggest that SWRT, both alone and in combination with mycorrhiza, significantly enhanced shoot elongation in argan seedlings. This finding aligns with recent studies, such as Lahbouki et al. (2022), which reported that SWRT improved shoot height in tomato plants. This growth boost could be attributed to improved soil fertility, as observed in the increased levels of available phosphorus (AP), total nitrogen (NTK), and organic matter (OM), along with improved soil structure. These factors reduce water and nutrient loss through percolation, creating an environment that supports robust plant growth processes.

Similarly, the parameters Fv/Fm (maximum photochemical efficiency of PSII) and stomatal conductance (gs) displayed seasonal trends, with the highest values recorded in SWRT- and M+SWRT-treated seedlings, whereas mycorrhiza-only treatments yielded the lowest values compared to the control. These results are in line with (Lahbouki et al., 2022), who also observed enhanced gs and Fv/Fm in tomato plants treated with SWRT under field conditions. Studies have shown that SWRT improves soil water retention and nutrient availability, providing a consistent supply of moisture and nutrients that boost stomatal conductance and aperture (Andrino et al., 2021; Figueiredo et al., 2021; Guber et al., 2015). Baslam et al. (2020) proposed that such improvements in physiological traits, including plant water status, enhance photosynthetic efficiency by enabling greater CO_2 uptake. Further supporting this, Naouraz et al. (2018) reported that AMF-inoculated plants, grown in hydrogel-amended soil, showed improved photosynthetic apparatus efficiency under drought conditions. AMF inoculation enhances PSII efficiency and gs compared to non-inoculated controls, corroborating findings from other studies (Liu et al., 2021; Wahid et al., 2020), which suggest that AMF can enhance water status under drought conditions. Ye et al. (2022) found that Fv/Fm in AMF-inoculated grapevines increased by 40% under water scarcity compared to non-inoculated plants. This mutualistic relationship is particularly beneficial under water-deficit conditions, as seen in various tree species like date palms (Toubali et al., 2020), grapevines (Ye et al., 2022), and cocoa (Seutra Kaba et al., 2021), where AMF improved growth, physiology, and nutrient uptake. Additionally, AMF associations increase root size, stomatal conductance, and gas exchange, helping plants better manage stressful climatic conditions. AMF also modulate abscisic acid (ABA) responses, which regulate plant physiology and stomatal activity, allowing AMF-associated plants in arid environments to adapt through

morphological, physiological, and biochemical responses. Moreover, AMF release glomalin, a glycoprotein that enhances soil structure and plant-soil water relations, fostering improved stomatal conductance and photosynthetic efficiency (Khaliq et al., 2022).

This study's findings suggest that SWRT, alone or combined with arbuscular mycorrhizal fungi (AMF), significantly enhanced chlorophyll and carotenoid contents in Argania spinosa seedlings. These results align with findings by Lahbouki et al. (2022), who observed increased photosynthetic pigment content in SWRT-treated tomatoes, attributing this to improved soil moisture similar to what was observed here. AMF inoculation further supported chlorophyll retention in arid conditions, which Zhu et al. (2012) and Zaouchi et al. (2015) have shown to improve photosynthetic efficiency and mitigate the negative effects of drought on the photosystem II (PSII) reaction center. Enhanced phosphorus and nitrogen uptake, promoted by AMF, likely contributed to this increase in photosynthetic pigments in AMF-treated seedlings (León-Sánchez et al., 2020). Our study also revealed that SWRT and AMF enhanced the content of osmoprotective compounds like proteins and soluble sugars. This accumulation is essential for maintaining cell integrity, osmotic balance, and protection from dehydration and oxidative damage under water stress (Liu et al., 2021; Toubali et al., 2020; Ye et al., 2022). Similar results were reported in previous studies on tomato and cactus, where SWRT positively affected protein content and promoted sugar accumulation under water deficit conditions (Del Buono, 2021; Lahbouki al., 2022). These findings support the idea that osmotic adaptation, through the accumulation of organic solutes, is a key mechanism for maintaining turgor pressure and reducing oxidative stress in drought conditions (Sharma et al., 2012).

Drought stress typically leads to an increase in reactive oxygen species (ROS), resulting in oxidative damage marked by elevated levels of malondialdehyde (MDA) and hydrogen peroxide (H_2O_2). The study found that SWRT, alone or combined with AMF, significantly lowered MDA levels, which is consistent with Lahbouki et al. (2022), who found SWRT application reduced oxidative stress in tomato by improving soil water retention. AMF further reduced MDA and H_2O_2 levels, as seen in studies on grapevine (Ye et al., 2022) and other species (Zaouchi et al., 2015; Zhu et al., 2012), likely due to its ability to enhance water uptake and nutrient availability, which counteract ROS accumulation and membrane damage. Lower MDA and H_2O_2 concentrations in treated seedlings indicate reduced oxidative damage, which Boutasknit et al. (2024) also noted under drought conditions.

To counter ROS, plants activate antioxidant enzymes like polyphenol oxidase (PPO) and peroxidase (POX). These enzymes help maintain ROS balance by converting superoxide radicals and H2O2 into less harmful molecules (Fang & Xiong, 2015; Nkurunziza et al., 2019; Sharma et al., 2012). The study demonstrated significantly higher PPO and POX activities in M+SWRT-treated seedlings, which is consistent with (Boutasknit et al., 2021) and recent findings in cactus (Lahbouki et al., 2022) showing SWRT increased antioxidant enzyme activity. According to (Dumanović et al., 2021), heightened antioxidant enzyme activities improve ROS scavenging efficiency, enhancing plant resilience to water scarcity.

1.5. Implications for policymakers

The results of this study provide the local policymakers with practical evidence to strengthen national reforestation and climate adaptation strategies. By demonstrating that Subsurface Water Retention Technology, native Arbuscular Mycorrhizal Fungi, and their combination significantly improve argan seedling survival and soil quality under arid conditions, this research highlights cost-effective tools that can be scaled up within programs and initiatives in the Argan Biosphere Reserve. Incorporating these techniques into reforestation projects would enhance water use efficiency, reduce seedling mortality, and secure the socio-economic role of argan ecosystems for rural communities, particularly women's

cooperatives. Furthermore, adopting these innovations would align Morocco's land restoration policies with its commitments to combat desertification and safeguard biodiversity.

1.6. Conclusion

This study demonstrates the significant benefits of SWRT and its combination with AMF on the growth, physiological, and biochemical responses of *Argania spinosa* seedlings. These treatments notably enhanced plant height, stomatal conductance, chlorophyll fluorescence, photosynthetic pigment levels, and antioxidant activity. SWRT also improved soil moisture at various depths, especially at 40 cm, and increased soil nutrient availability, with the most pronounced effects when paired with AMF. These findings suggest that combining SWRT with AMF is a promising strategy to support argan seedling survival in harsh arid and semi-arid climates, making it a valuable approach for reforestation in argan ecosystems.

2. Tunisian Living Lab "JEFFARA"

2.1. Introduction and statement of the research gaps

The SALAM-MED project aims to identify, test, and validate practical solutions to enhance the resilience of threatened socio-ecological systems or to restore degraded ecosystems in arid and hyper-arid areas of the Mediterranean region. In Jeffara LL, It engages all relevant stakeholders to address knowledge gaps on MAR out-scalability, and assess eventual impacts on agricultural cropping patterns.

Thousands of years ago, the need to collect the surface water, to limit sediment's transportation and to enhance recharge in arid areas was already recognized by our ancestors. Traditional Water harvesting techniques (WHT) were then invented and they have been passed down from one generation to the next up until nowadays. The traditional WHT were *Jessour* and *Tabias*. The *Jessour* consist of a number of Jessr, which is a hydraulic unit installed at the talwegs of valleys, mountainous and gentle slope's areas. The Jessr is used not only to allow the retention of runoff water and sediments, but also to create rich agricultural areas, to conserve the vegetation cover and to recharge the aquifer. The Jessr is composed of three components: the Impluvium, the Terrace and the Dyke (colled also Tabia) (El Amami 1982, 1984). The impluvium or catchment is the area used to collect the rainwater. The terrace is then the cropping zone. The dyke is a wall in packed earth having between 2 to 5m as height and between 15 to 50 m as length across the wadi; it is also called Ketra or Tabia, (Ben Mechlia and Ouessar 2004). The dyke most often has spillways that can be either lateral (menfess) or central (massraf) to evacuate the excess water. *Tabias* are similar to the *jessour,* they are essentially situated on gentle slopes, in the piedmont surfaces and in the middle of the watershed. The *tabia* is formed by a principal embankment of 50 to 150 m situated along the contour with two additional lateral bunds of about 30m long at the ends (Alaya et al. 1993; Ouessar 2007). Other WHT are used in the study area, such as *Groundwater recharge structures* which are built in gabion across the wadis. The length of the recharge structure is almost equal to the width of the wadi bed and its height is variable from 2 to 3 m. They collect runoff water to promote infiltration and reduce flooding by breaking down the runoff rate. The recharging of aquifers by *recharge wells* is a technique used mainly for aquifers with calcareous structures presenting low permeability. They show a notable efficiency in recharge even with the naked eye during the observation visits. A *recharge well* consists of an inner long tube leading to the watertable or permeable layer and an outer tube at the surface fixing the gravel filter (Yahyaoui and Ouessar 2000; Yahyaoui et al. 2002; Ouessar 2007).

The present study emphasizes the role of the WHT and specially the recharge wells, in the recharge of the Triassic aquifer of "Sahel El Ababsa" located in the Tunisian LL, governorate of Médenine. It aims to enhance the capacity to identify practical solutions for sustainable water resources management (GDRES) in the targeted rural areas of the arid Mediterranean region. The WHT impact on the aquifer recharge is studied in this work with the next models: the linked SWAT-MODFLOW model and the WEAP model.

2.2. Materials and methods

2.2.1. Study Area

The Triassic aquifer of "Sahel El Ababsa" is a part of the Jeffara plain in the Tunisia South-Eastern region. It covers an area of 650 km^2. The majority of the extent area of the aquifer belongs to the governorate of Médenine (620 km²). A minor part of it belongs to the governorate of Tataouine, in the southern limit (30 km² representing approximately 5% of the total area of the aquifer). The main

watersheds of the studied aquifer are Koutine, Gattar and Hjar. They contain the whole cities of Koutine, Metameur and Médenine belonging to the governorate of Médenine. The study area has an arid climate where the average annual rainfall is about 180 mm with about 30 rainfall days per year. The water balance of the region is deficient throughout the year. The rainfall in the study region is characterized by low averages and spatio-temporal irregularity (Gaubi 1995; Yahyaoui 1996, 2001, 2007).

2.2.2. Experimental design

As the present study aims to to identify practical solutions for sustainable water resources management, a Conducting geophysical surveys were carried out using the electrical method.

The experimental design Consisted on:

- Manage of 3 existing recharge well in Koutine watershed to improve the recharge and to slow down the evaporation
- The use of the Electrical Resistivity Tomography
- Piezometric Monitoring of Aquifers: Equipment recharge wells and associated piezometers with sensors.
- Installing sensors at farmer's scale.
- Analyze data collected from the existing monitoring system.
- Collect data for modeling (WP3).

The data (rainfall, piezometric levels, climatic data, etc.) were collected from the IRA data platform. It is used to inform the Living Lab (LL) stockholders about the impacts on watersheds (surface and groundwater resources) and farmers (agricultural crops).

The use of the Electrical Resistivity Tomography aims to co-designing management plans (recharge sites, cropping systems, etc.) and procedures to leverage long-term benefits while ensuring technical efficiency and practical feasibility.

2.2.3. Electrical Resistivity Tomography

The determination of soil characteristics behind recharge structures by carrying out electrical resistivity profiles associated with topographic surveys is assumed to be an effective method for estimating sediment yield and assessing the efficiency of hydraulic infrastructure at different levels in small and medium-sized watersheds.

Gabion structures are very important recharge and flood control structures in the study area. This part aims to define the physical properties of the sediments deposited behind gabion structures distributed upstream, in the center and downstream of the study site. Detection of sediment features is based on electrical resistivity tomography (ERT), supported by soil analysis and topographic terrain surveys.

ERT measurements were performed using Syscal Junior/R1+ developed by IRIS Instruments (IRIS, 2012). The instrument consists of a multi-electrode system equipped with a control unit to run 2D electrical resistivity profiles. The system consists of a central processing unit encompassing a current transmission and a potential voltage receiving unit, and has several switches that allow 72 stainless steel electrodes to be connected to transmit current and to measure the voltage potential to any combination of four electrodes along the profile. To collect the electrical resistivity data, 72 electrodes

were used and aligned in a 2D profile. Sequence parameters can be pre-programmed using Syscal's Electre Pro software to determine the optimal electrode array type, electrode spacing, and depth penetration required for the study objectives. The Schlumberger-Wenner electrode array was used with electrode spacing ranging from 0.5 to 4 m, depending on the required penetration depth.

The electrical resistivity profiles are made on about ten lines by adopting the wenner-schlumberger device with different configurations and using 72 electrodes that have been planted and arranged in a straight pattern along the measurement profile (Figure 9). The use of the Wenner-Schlumberger device is recommended for land upstream of gabion structures that have both horizontal and vertical structures. It is generally a low-noise device and allows the acquisition of a larger number of points.

The resistivity data was reversed using the Res2Dinv program (Aarhus-GeoSoftware, 2022). Soil samples are taken for analysis in the laboratory and used to calibrate the calculated values.

Figure 9. Electrical resistivity measurement devices (ERT)

To assess the impact of gabion structures, ERT profiles are carried out at different points in the catchment area (upstream, centre and downstream). However, the location of the profiles was chosen in the reservoir of the well structure in order to help quantify the sediment input. Electrical resistivity profiles were carried out at many sites in locations (Figure 2). For all electrical resistivity profiles, 72 electrodes were used with a variable electrode spacing survey line of 0.5 to 4 m, resulting in length profiles between 36 and 288 m.

2.3. Results

2.3.1. Example of an electrical resistivity tomography profile

The resistivity of soils tends to decrease as porosity increases. However, resistivity does not always correspond to porosity, even in the same soil type, due to different mineral compositions and pore geometries. The resistivity of rocks increases with the increase in the resistivity of the fluid, regardless of the type of soil. However, between 20 and 100 ohms m, which is the available resistivity of water in rock masses, the resistivity of fluids has little effect on the resistivity of soils. This resistivity decreases with increasing water saturation. In addition, for unsaturated soils, it increases exponentially with the decrease in water saturation. The direct relationship between permeability and electrical resistivity is mainly due to surface conductivity which decreases as the soil becomes coarser (Figure 10).

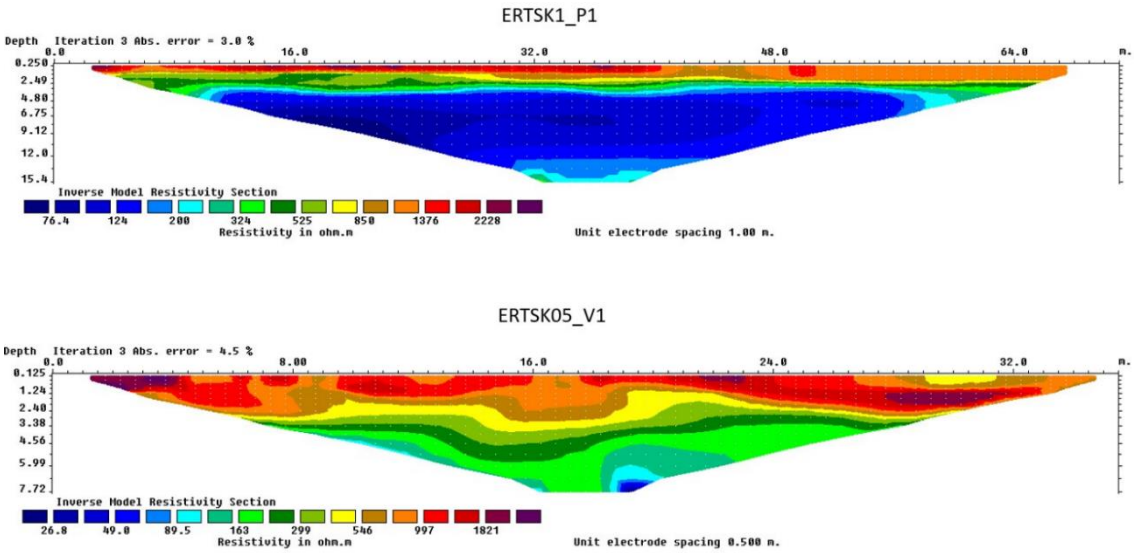

Figure 10. Example of an electrical resistivity tomography profile

The results of the ERTs and the particle size analysis in the reservoirs of the gabion structures show the presence of sediment deposition (caused by erosion processes at the basin scale) with a thickness that varies from 1 to 3 meters. In the majority of electrical prospecting sites, the top layer shows a fine texture in addition to high electrical resistivity and consequently low hydraulic conductivity of the retention basins. Interpretation of resistivity values indicates spatial and temporal variability in the physical properties of the soil. These results will be beneficial for decision-makers to evaluate the performance of recharge structures and appropriately manage soil resources based on scientific evidence.

In the presence of a large number of recharge structures, erosion at the scale of the catchment area causes a significant sedimentary deposition which significantly reduces the efficiency of these gabion structures. Indeed, to increase permeability at the level of the recharge sites, it would be useful to carry out periodic cleaning of the reservoirs to move the surface layer which has a high resistivity in addition to its fine texture. On the other hand, tillage (holding planting) could be a beneficial solution both for recharge and economically (improved income) for farmers in the vicinity. Finally, the installation of existing filter wells with refill chambers and the creation of other filtering wells will increase infiltration remarkably and reduce the volumes of water evaporated from the retention basins.

2.3.2. Creation of recharge chamber

During the second year of the project three existing recharge chamber was managed by recharge chamber based on the electrical resistivity measurement (figures 11 and 12) in order to:

- Increase infiltration around the recharge well.
- Improve the filtration system.

2.3.3. Dimension of recharge chamber

The purpose of the recharge chamber is to increase the efficiency of artificial groundwater recharge through the recharge well. It carried out after the well has been completed. The recharge

chamber is rectangular in shape, with a center corresponding to the recharge well and the large transverse side in relation to the direction of the flow in the wadi. The planned dimensions are 10x20 m (Figure 11) but they may vary depending on the width of the wadi in the site where the charging chamber will be built.

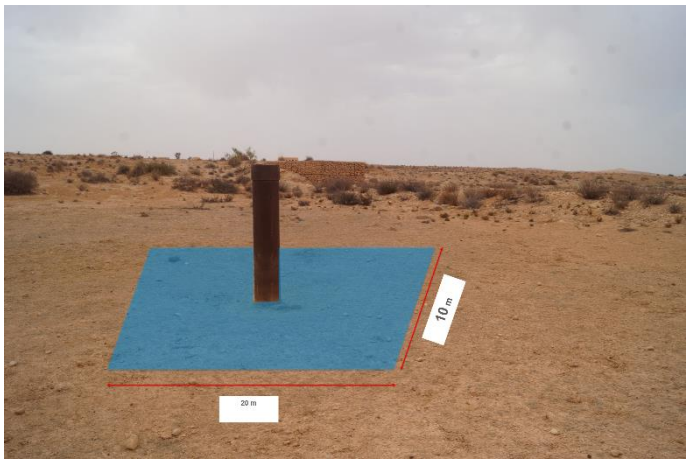

Figure 11. Recharge chamber concept

Figure 12. Realization of recharge chamber

2.3.4. Excavation

The height of the chamber is 2.50 m at the deepest point of the excavation, in correspondence with the recharge shaft, and 1.80 m in correspondence with the wall of the excavation (Figure 13), in order to give the bottom of the excavation the necessary slope. The excavation will be carried out by means of an excavator, which is accessible through the construction of a ramp.

The bottom of the chamber will not be waterproofed. This design choice increases the efficiency of aquifer recharge, as it allows the percolation of the recharge chamber to the Triassic aquifer through the Quaternary alluvium. These water inputs arrive at the aquifer affected by the artificial recharge at a delayed time compared to the direct inputs that occur through the recharge well.

The excavation will be filled to a depth of 0.40 m from ground level with two superimposed layers consisting of, from bottom to top, by:

- a layer of gravel recovered in situ, which, in correspondence with the wall of the excavation, will be 0.90 m thick;
- a layer 0.90 m thick represented by a Passive Treatment System (Figure 14).

Both layers have a function of filtering suspended and dissolved inorganic matter and promote the degradation processes of organic contaminants in order to improve the quality of the water that recharges the aquifer.

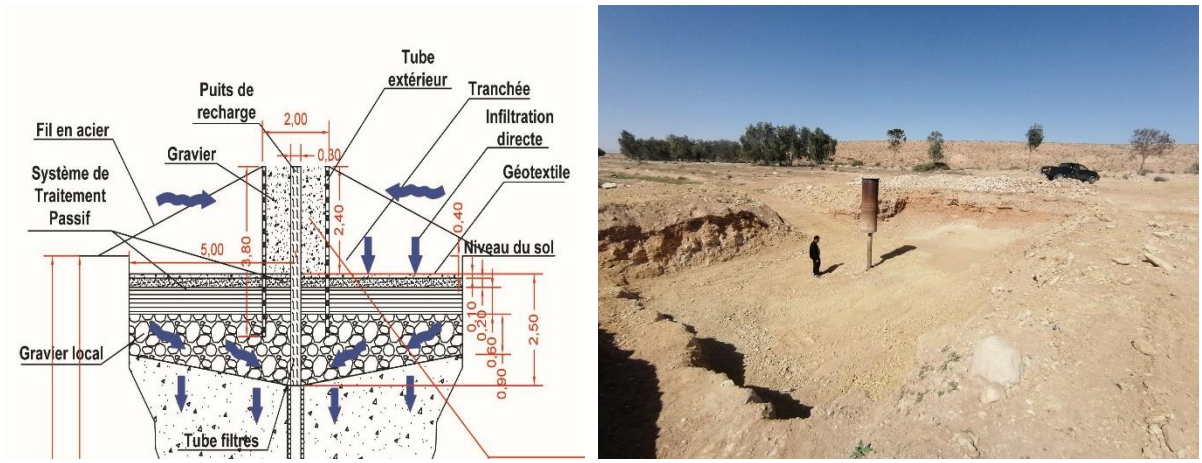

Figure 13. Excavation wall

2.3.5. Passive Treatment System

The installation of the Passive Treatment System is based on the experience gained by the University of Barcelona in the framework of the Life+ ENSAT project (Improvement of the treatment of the ground aquifer) (http://www.life-ensat.eu/), during which an artificial recharge system was developed, consisting of recharge basins, located in Sant Vicenç dels Horts, in the lower Llobregat Delta (Catalonia, NE Spain). For the design of the Passive Treatment System, previous laboratory work was done to select an appropriate material to improve the biodegradation processes of contaminants present in the recharge water from the Llobregat River.

In the Passive Treatment System, the reactive layer will be about 0.60 m thick and is composed of a mixture of aquifer gravel material (50% by volume), autochthonous plant compost represented by crushed palm leaves (49% by volume) and minor clays (1% by volume). These components are amalgamated with a shovel until a relatively homogeneous mixture is obtained. This layer will be covered with about 20 cm of sand and 10 cm of gravel, in order to prevent the material from floating before being dispersed with the iron oxides in the form of goethite (0.1% by volume) and to protect the underlying layer from erosion (Figure 6). In the reactive layer, the aquifer gravel, starting from the trench, will give structural integrity and ensure hydraulic conductivity. The purpose of plant compost is twofold: 1) to release DOC, which would encourage microbial growth and promote several redox conditions to induce denitrification; 2) provide additional sorption sites for neutral contaminants. Clays (mainly consisting of 33% illite, 16% smectite and 9% chlorite) and fine-grained iron oxides that could provide better sorption capacity for cationic and anionic contaminants, respectively.

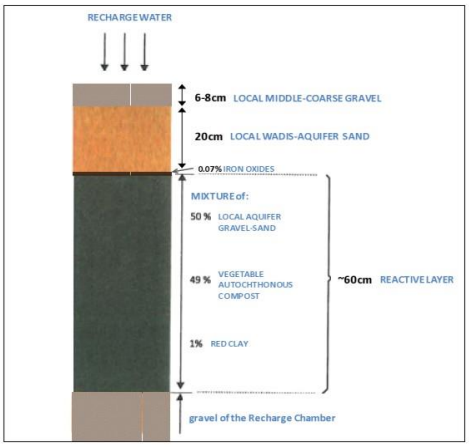

Figure 14. Passive Treatment System

2.4. Data collection

2.4.1. Weather station

In order to control climatic data at real time for irrigation practices and modelling purposes, a weather station was installed in the study site (Figure 15) and connected with IRA platform (Figure 16).

Figure 15. Weather station

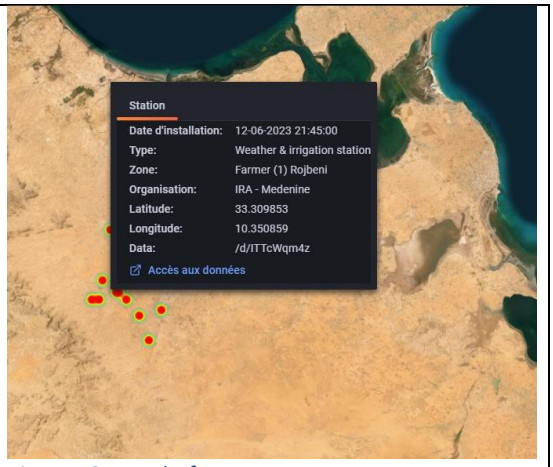

Figure 16. IRA platform

From the installation of the weather station in June 2023 until December 2024 we registered only four events in which the rainfall is more important than 20 mm and generates runoff. The maximum reached 40 mm.

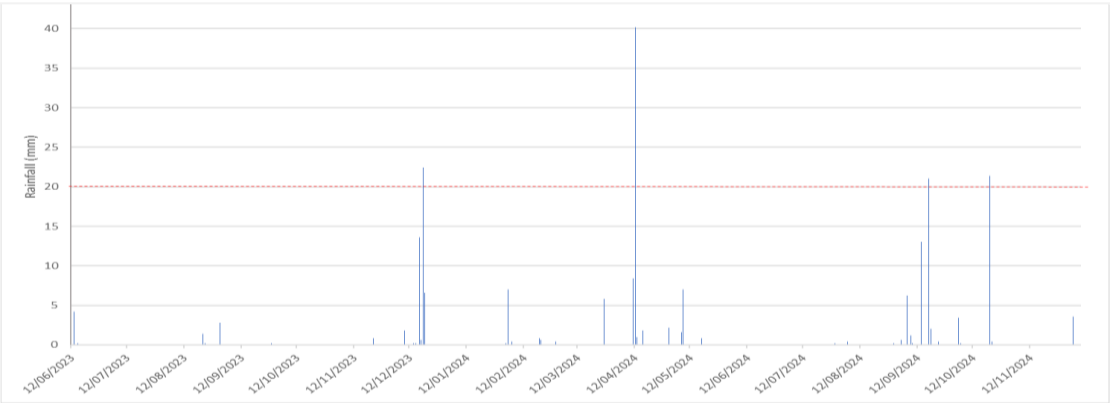

Figure 17. Collected Rainfall data (June 2023-December 2024)

The selected weather station is composed by two axes Ultrasonic Anemometer and rain gauge with tipping bucket 200 cm^2 to monitor the main meteorological variables such as air temperature, relative humidity, radiation, and precipitation (Figure 18).

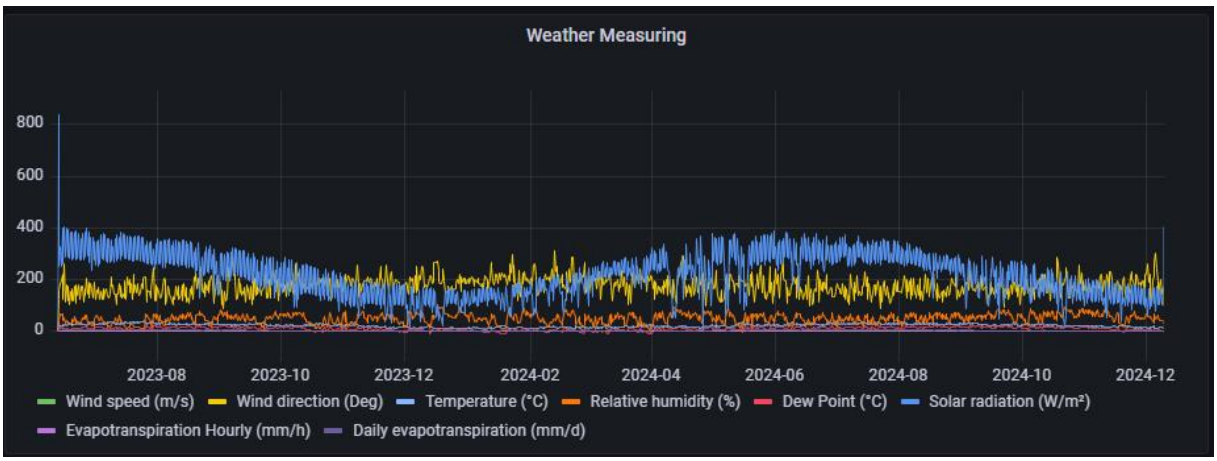

Figure 18. Main monitored meteorological variables

2.4.2. Piezometric and water quality data

At the watershed level, sensors for water level and quality were installed in defined monitoring points (Figure 19):

- One piezometer located in Hjar(33°14’45”N 10°26’40”E) was equipped with Aqua Troll 500 sensor for monitoring water level.
- One piezometer located in Guattar (33°20’24”N 10°24’58”E) was equipped with Huba Control level sensor for monitoring groundwater water level.
- One piezometer located in Megarine (33°19’06”N 10°22’48”E) was equipped with Huba Control level and Aqua Troll 500 sensors for monitoring water level and quality
- One recharge well located in wadi Arnième was equipped with Huba Control level and Aqua Troll 500 sensors for monitoring water level and quality

The installation of these equipment’s was in February 2024.

Figure 19. Installed sensors for water level and quality

The measured data are transmitted instantly to IRA Data platform (Figure 20)

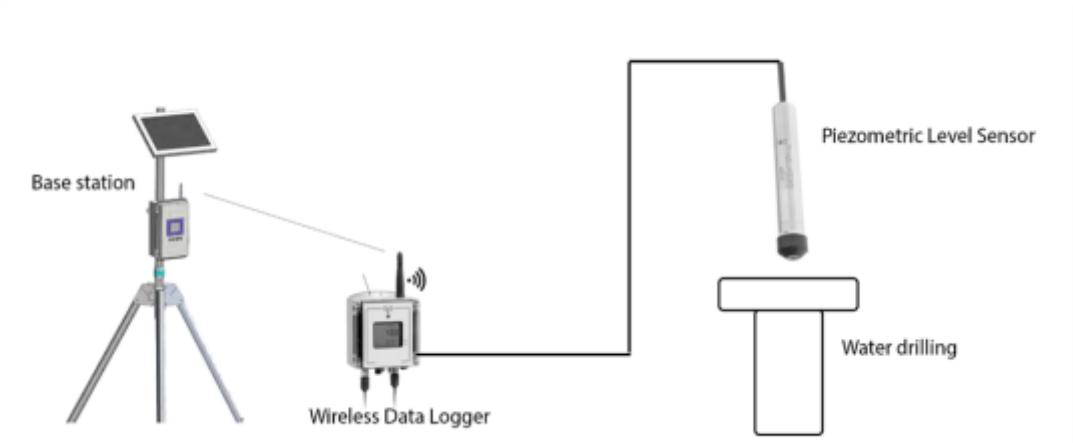

Figure 20. Installation structure for piezometric level

The base unit (GSM gateway) and the wireless data logger are connected via radio frequency for wireless communication. On the other hand, the piezometric level sensor and the wireless data logger for water level are connected by a cable for data transmission.

2.4.3. Water sampling for quality analysis

The study investigates groundwater quality in the Triassic sandstone aquifer of southeastern Tunisia, addressing issues of water scarcity, illegal exploitation, and climate change impacts. A sampling campaign was conducted, collecting 19 water samples. The research utilized Geographic Information Systems (GIS) to analyze spatio-temporal variations in various groundwater parameters. The methodology included geochemical and isotopic analyses to assess water quality and determine the aquifer's recharge origins (Figures 21 and 22).

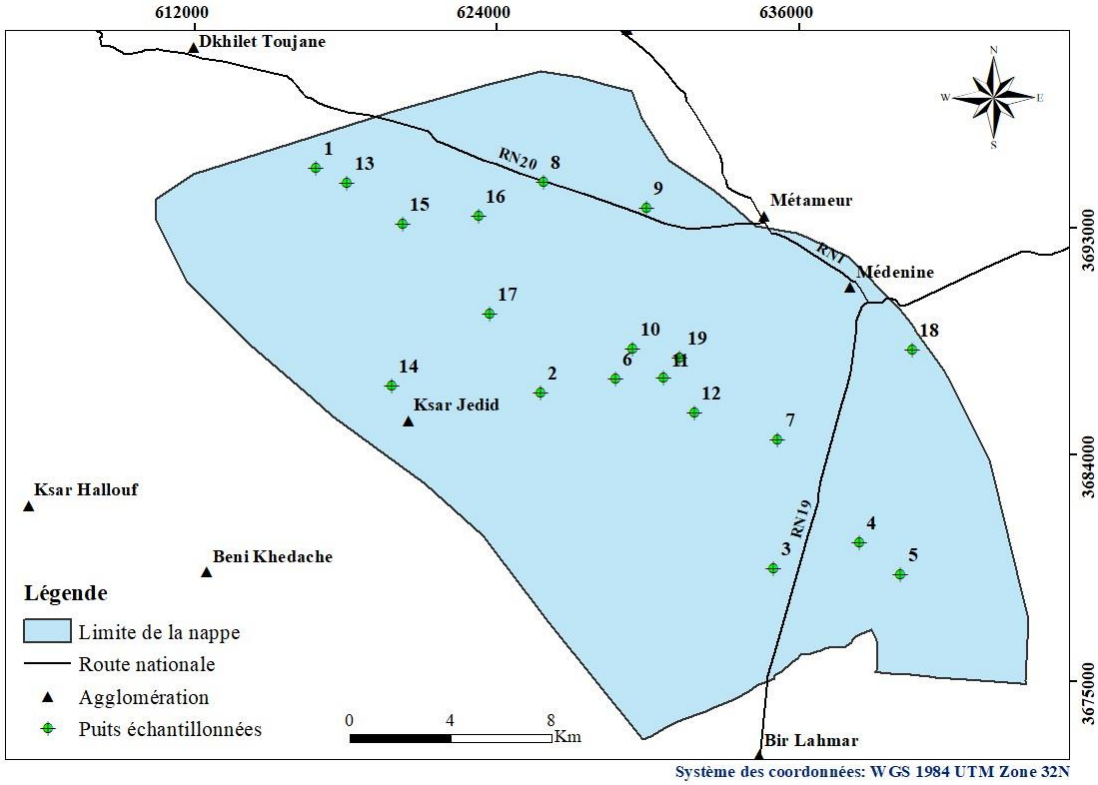

Figure 21 : Map of the location of wells sampled in the aquifer

The results indicate significant sodium (44%) and sulfate (46%) ion enrichment in the groundwater, leading to a predominance of sodium sulfate facies. The mineralization is primarily influenced by chloride and sodium ions, with a positive correlation observed. Water quality deteriorates from southwest to northeast, with 53% of the samples classified as good quality, 16% as poor quality, and 31% as very poor quality. The isotopic analysis revealed that the aquifer is primarily fed by a complex recharge system, influenced by regional geology and local climatic conditions.

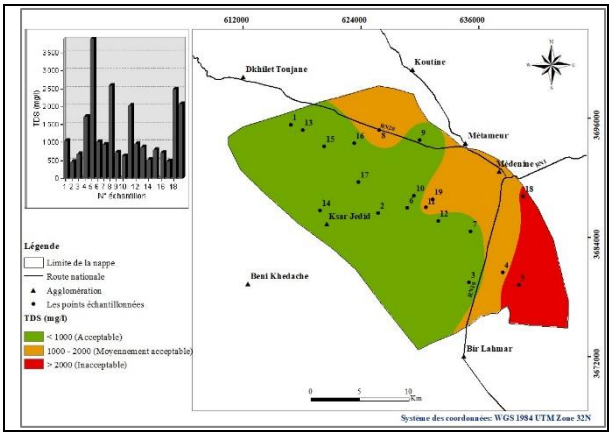

spatial distribution map of Total Dissolved Solid (TDS)

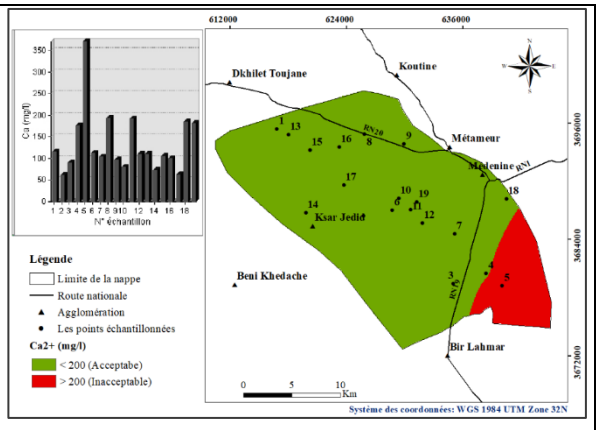

Spatial distribution map of calcium

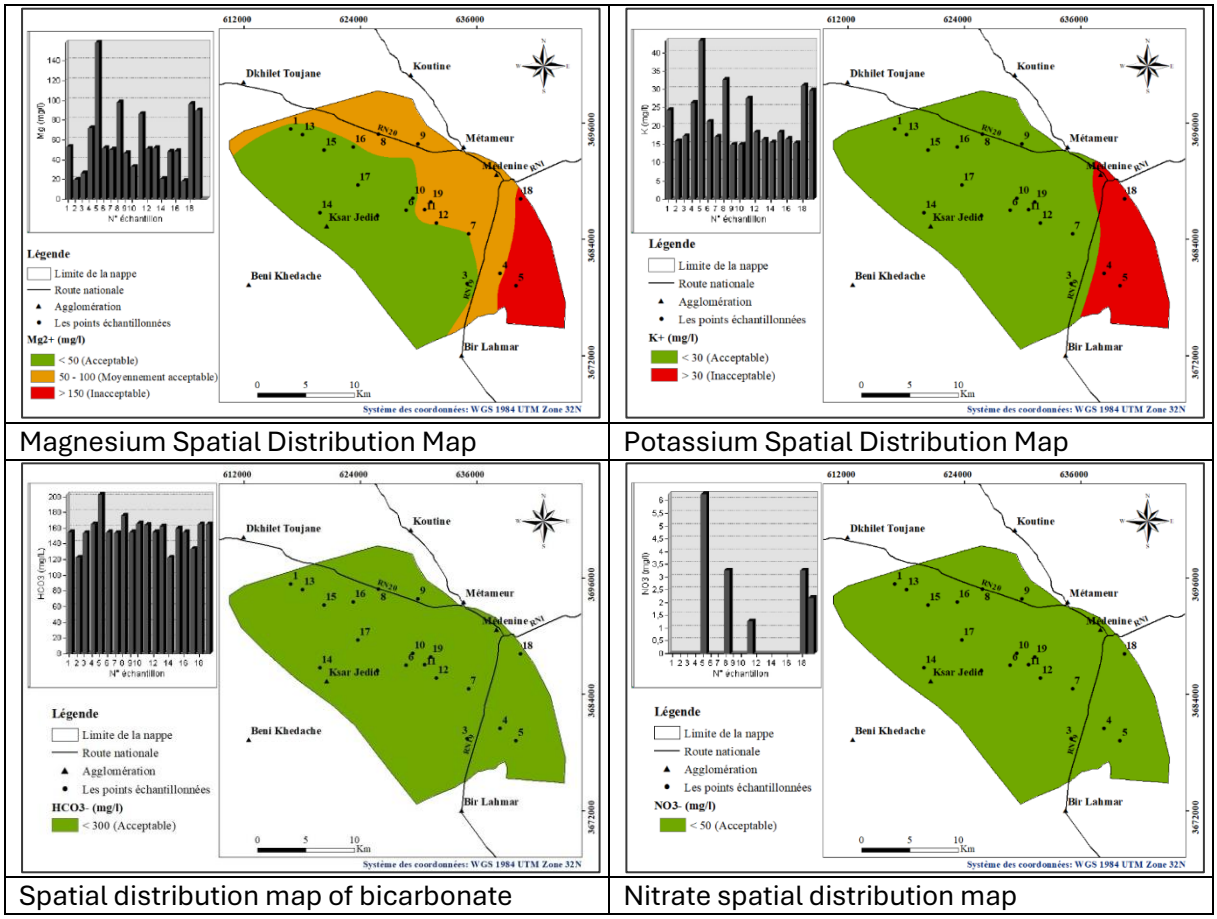

Magnesium Spatial Distribution Map | Potassium Spatial Distribution Map

Spatial distribution map of bicarbonate | Nitrate spatial distribution map

Figure 22. Spatial distributions of pollutants

2.4.4. Data Collection and Visualization

The data collection server receives encrypted data from devices using either the HTTP or FTP protocol. The server then decrypts the data using specific software and stores it in a SQL database.

After collecting the data from the database server, the next steps involve visualizing the data with a web server (Figure 23).

Figure 23. Visualization of collected data

2.4.5. Elaboration of landuse map

The landuse map was developed based on *Landsat TM image dated September 22, 1984*, 30m spatial resolution. Supervised classification using the CART algorithm in Google Earth Engine (Figure 24). The soil map is updated from previously study of Taamallah 2003, modified by Ouesssar 2007, 2023 (Figure 25). Crops data are collected from previous study in the region (Ouessar 2007), the Olive trees are the dominating fruit trees cropped in the area. They are generally planted on the terraces of jessour and tabias to profit from the additional collected runoff water and the relatively deep soils formed as a result of the accumulation of sediments. The characteristics of the US southwest rangelands were used with minor adjustments (biomass production, grazing pattern, base and optimal growth temperature) based on research work undertaken in the arid regions of Tunisia (Floret and Pontanier 1982; Neffati 1994; Ouled Belgacem 2006). While the cereal crop parameters suggested by Bruggeman and Van der Meijden (2005) for the Khanasser Valley (Syria) were adopted because of similar climatic dryland conditions (Ouessar 2007; Ouessar et al. 2009).

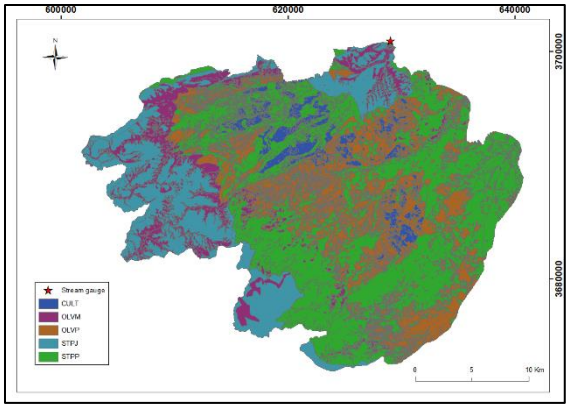

Figure 24. Adjusted land use map (year 1984)

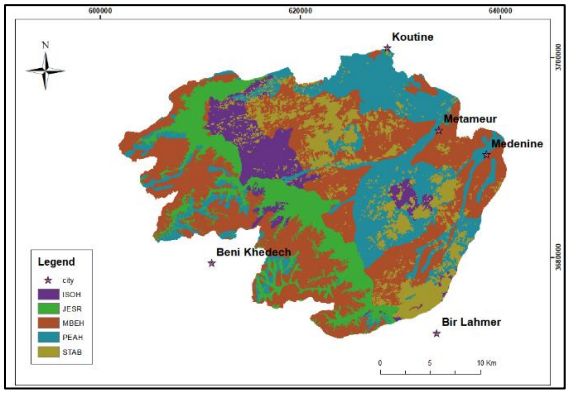

Figure 25. The updated soil map for modeling purp

2.5. Discussion

Traditional jessour and tabias retain runoff and sediments, create fertile micro-zones for cropping, conserve vegetation, and contribute to local recharge. They remain culturally embedded and spatially distributed on talwegs and piedmonts. These systems provide multiple co-benefits (soil, vegetation, local recharge) but their effectiveness for aquifer-scale recharge is heterogeneous and limited by sediment accumulation and fine surface layers that reduce infiltration. Thus, traditional WHT are valuable for localized resilience but require complementary measures for landscape-scale MAR.

The ERT and particle size analyses show 1–3 m of sediment deposited behind gabions; top layers are often fine textured with high resistivity and low hydraulic conductivity. Sediment deposition is spatially variable across upstream/center/downstream locations. The accumulated fine sediments severely reduce permeability of recharge basins, lowering infiltration rates and hence MAR efficiency. The presence of a large network of recharge structures accelerates catchment-scale sediment trapping, creating the paradox where sediment control structures progressively impair recharge unless periodically de-silted or coupled with upstream erosion control.

Managed recharge wells (including new recharge chambers sized ~10×20 m with reactive filter layers) and filter wells with refill chambers increased observable infiltration. Design intentionally left non-waterproofed bottoms to enhance percolation through Quaternary alluvium. Passive Treatment System (PTS) reactive layers (gravel + palm compost + minor clay) aim to improve water quality and promote denitrification. Combining recharge wells with adjacent recharge chambers and PTS increases contact area and residence time, improving both volumetric recharge and water quality improvement. However, their performance depends on upstream sediment load (which can clog surface filters), proper material selection and maintenance of the PTS, and matching hydraulic connectivity to the Triassic aquifer.

The installed weather station (since June 2023) recorded only four runoff-generating rainfall events (>20 mm) through Dec 2024, the largest at 40 mm. Piezometers and quality sensors installed Feb 2024 transmit data to the IRA platform in real time. The low frequency of runoff events constrains opportunities for episodic recharge; MAR systems will depend on infrequent high-magnitude events. Real-time monitoring provides critical data to link storms to aquifer response but the monitoring period remains short — longer datasets are needed to robustly calibrate models and infer long-term recharge under variable climate.

Groundwater shows dominant sodium-sulfate facies (Na and SO4 enrichment), spatial deterioration from SW to NE, and 53% of samples as good quality, 16% poor, 31% very poor. Isotopic analysis suggests complex recharge origins influenced by regional geology and local climate. The artificial recharge risks altering aquifer chemistry if recharge water carries salts or contaminants; the PTS design addresses some organic and nutrient concerns but saline loads (Na, Cl, SO4) are structural issues. MAR design must account for pre-existing salinization gradients and selective placement where dilution and natural attenuation are sufficient.

The water quality analysis highlights the implications of declining water quality and its potential impacts on soil properties and agricultural practices. The research emphasizes the importance of understanding the geochemical and isotopic composition of groundwater for effective water management. The findings indicate that the aquifer's quality is deteriorating mainly due to anthropogenic factors, exacerbated by natural climatic variations.

Modelling was used to estimate WHT impacts on recharge and cropping patterns (details not fully reported in the text excerpt). Numerical models are essential to evaluate future scenarios and up-scalability of MAR; nevertheless, model outputs are sensitive to uncertainties in sediment dynamics, episodic rainfall forcing, and short monitoring records. Model validation with longer-term piezometry, tracer tests and sediment budgets is necessary before confidently up-scaling MAR strategies.

Positive outcomes: WHT and engineered recharge increase local infiltration, support crops (e.g., terraces for olives), and can improve water quality when coupled with PTS. Monitoring infrastructure enables near-real-time assessment and adaptive management.

Limiting factors: Sediment deposition reducing permeability, low frequency of recharge events, background salinization, maintenance requirements, and limited monitoring duration constrain both efficiency and reliable up-scaling.

Adaptive pathway: Combine upstream erosion control, targeted placement of recharge wells/chambers where geology favors connectivity, and maintain passive treatment for water quality. Use models iteratively with expanding monitoring datasets to reduce uncertainty.

2.6. Implications for policymakers

Policymakers view MAR and WHT in Jeffara as complementary, locally beneficial interventions that can enhance resilience only if embedded within an integrated catchment strategy. Key policy implications are: prioritize funding for (1) systematic maintenance (regular de-siltation and rehabilitation) of gabion and recharge structures to prevent progressive loss of infiltration capacity; (2) installation and long-term support for monitoring networks (piezometers, weather stations, water quality sensors and telemetry) and tracer studies to validate modelled recharge and water-quality trajectories before large-scale up-scaling; (3) upstream erosion control and land-management incentives (vegetation restoration, contour farming, reduced bare soil exposure) to reduce sediment delivery to recharge sites; (4) selective siting of recharge chambers and wells in locations with favorable hydraulic connectivity and lower background salinity, coupled with Passive Treatment Systems to manage organic/nutrient contaminants; (5) integration of MAR plans into agricultural support schemes (training, cost-sharing for maintenance, promoting crop systems that maximize recharge benefits without degrading soils); and (6) adaptive governance mechanisms that link local stakeholders, scientists and water agencies to iteratively update designs based on monitoring and modelling outcomes. Addressing these priorities will close critical research and implementation gaps and increase the likelihood that MAR interventions provide sustained hydrological and socio-economic benefits in arid Mediterranean landscapes.

The study's findings underscore the need for effective water management strategies and policies to protect groundwater resources in the context of increasing demand and environmental stress. Policymakers are urged to consider the geochemical characteristics and quality assessments in decision-making processes related to irrigation and water resource management, aiming to mitigate adverse effects on agriculture and ensure sustainable water use in the region.

2.7. Conclusion

The Jeffara Living Lab study highlights the effectiveness of traditional water-harvesting techniques (jessour, tabias) and engineered structures (gabions, recharge wells, chambers with Passive Treatment Systems) in improving groundwater recharge, soil conservation, and agricultural productivity in the

arid Sahel El Ababsa aquifer. Field investigations and monitoring confirm that recharge chambers enhance infiltration and passive layers improve water quality. Yet, limitations arise from sediment accumulation, reduced infiltration due to fine layers, and the scarcity of runoff-generating storms, which constrain recharge opportunities. Groundwater chemistry, dominated by sodium-sulfate facies, poses risks of increased salinity, demanding careful siting. Scaling up requires integrated action: upstream erosion control, systematic maintenance, targeted siting of recharge structures, and expanded Passive Treatment Systems. Sustained monitoring via piezometers, tracer tests, and sediment budgets—remains crucial to reduce uncertainties and validate models. For policymakers, MAR and WHT should be seen as complementary within a catchment strategy, supported by adaptive governance and stakeholder engagement. Investment in maintenance and long-term monitoring will ensure socio-ecological benefits, including improved infiltration, crop support, and better water quality management. Ultimately, resilience in arid Mediterranean systems depends on combining MAR, WHT, and engineering solutions with erosion control, maintenance, and long-term adaptive management.

3. Egyptian Living Lab "Matrouh"

3.1. Introduction and statement of the research gaps

Climate change affects the world's water in complex ways (e.g., water scarcity and water-related hazards), where many problems and challenges, such as soil salinization, waterlogging, and soil degradation, have been accelerated. Changes in climatic patterns (e.g., frequency and intensity of precipitation, humidity, temperature) are expected to significantly affect terrestrial systems, soil properties, surface water and stream flows, causing high levels of uncertainty in climate model projections, at both regional and local scales. Within this context, accurate soil hydraulic and transport characteristics become a necessity (Dragonetti et al., 2022).

The moisture content of soil is a measure of the amount of water in a unit soil volume. It plays a very important role in many parts, like agriculture, geotechnical engineering, and geology. For agricultural purposes, moisture content is one of the most important parameters that affect plant growth. Also, water soil content has an important impact on engineering properties of soils, such as volume changes, compressibility, and shear strength for geotechnical engineering. Generally, the determination of water content is an important measure that is used for the investigation of soil samples' characteristics.

There are different experimental methods and sensors for measuring water content. For field applications, indirect methods are generally used, such as Time Domain Reflectometry (TDR), which measures the dielectric constant of soil, from which the water content may be estimated through a specific calibration curve. However, for large scale applications, other less-invasive or even non-invasive geophysical techniques are more and more used, such as Electrical Resistivity Tomography (ERT) and Electromagnetic Induction (EMI). Recently, due to advances in geophysical instrumentation and interpretation algorithms, the use of geophysics in agricultural research has seen a rapid expansion, as an emerging agricultural geophysicist seeks to help understand soil heterogeneity by identifying spatial patterns of petrophysical parameters and relating them to hydrological properties or states. Indeed, the ability to reliably predict the soil properties of subterranean formations using a non-destructive instrument is one of the most important and challenging goals in hydrogeophysics (Figure 26, Binley et al., 2015).

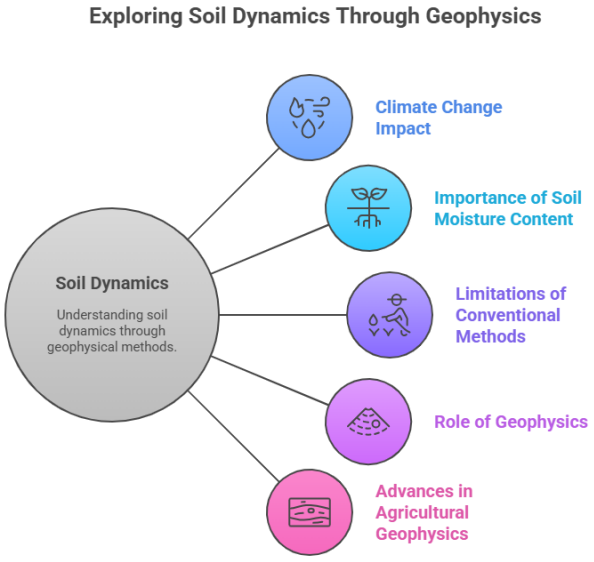

Figure 26. Principles of hydrogeophysics

The application of these techniques and related sensors has proved to be particularly useful for the monitoring activities, to be carried out within the **Task 2.3 Practical solutions to restore degraded lands.** Actually, they have been used for the soil and hydrological characterization of some sub-basins of the wadi Kharrouba, needed for understanding the hydrological behavior of the wadi and its potential for agricultural exploitation.

In any case, the use of these techniques must be based on direct soil measurements for their calibration and validation. In this context, many field trips have been conducted to carry out field measurements and soil sampling processes, gathering clear and accurate information about the chemical and physical soil characteristics. This information will be used in successive versions of the SALAM-MED project database and considered important input data for surface hydrological and agro-hydrological modeling. Also, nine infiltration tests have been carried out to identify the hydraulic conductivity of the soil, which will also be used in the modelling analysis.

Preliminarly, due to the sedimentation processes resulting from the successive runoff in rainy seasons and the absence of maintenance processes for the levelled terraces and dikes, maintenance and rehabilitation processes for six main dikes in the Wadi Agarma, a sub-basin of the wadi Kharrouba, have been carried out to restore the degraded agricultural terraces before carrying out the hydrological characterization.

3.2. Materials and methods

SALAM-MED capitalizes on the soil and hydrological characterization already available at the Wadi Kharrouba (EG) to provide new experimental evidence on wadi hydrology and the potential for agricultural exploitation. Also, soil samples and field experiments are performed for the modelling, as well as for the database repository of the SALAM-MED project.

From 27/12/2022 to 3rd of January 2023, a field trip was carried out to Wadi El Agarma, El Safa, and El Ramal to carry out some field measurements for the dikes' dimensions and infiltration test (Figure 27) in the 3 catchments, besides soil sampling for chemical and physical analyses in the laboratory. Also, during this field trip, inspection of the dikes in the wadies was carried out to identify how many dikes require maintenance, and already 6 main dikes have been determined for rehabilitation.

Figure 27. Field photo during the experiment of infiltration test at Wadi El Agarma

To advance the work of Task 2.3, several field and laboratory measurements, focusing on Soil Moisture Content, including:

- Perform Laboratory-scale soil moisture Measurements

- Soil moisture measurements were performed at various depths within the soil profile
- Perform Soil Moisture Content Using Geophysical Techniques, including:
  - Electrical Resistivity Tomography (ERT)

3.2.1. Study Area

The selected test site is one of the tributaries of the Wadi El Agarma sub-basin, which is considered a sub-basin of Wadi El Kharouba on the north-western coast of Egypt at Matrauh Governate (Figure 28). In this location, six levelled terraces were prepared and reclaimed to be cultivated by olive and fig trees. Two terraces out of six are not cultivated. One of these terraces was chosen to be the test site for cultivating olive seedlings in order to apply the Microbial consortia during the transplanting processes. The surface area of the cultivated terraces is 1434 square meters. Twenty-eight olive seedlings had been transplanted in the selected location in the form of three lines in two terraces.

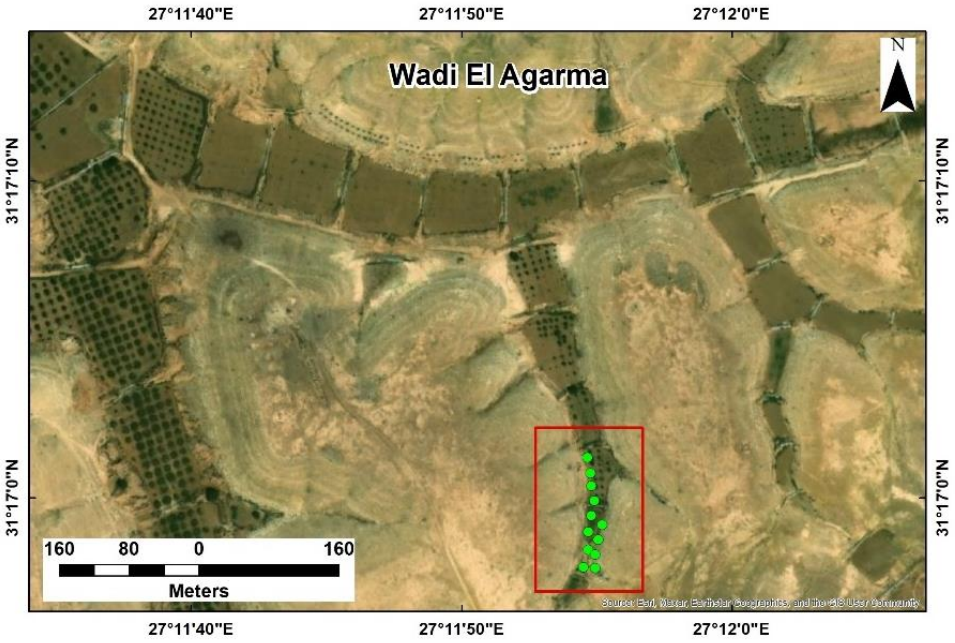

Figure 28. Location map of Wadi Agarma catchment

Wadi basins are typical of arid or semiarid regions (Wheater, 2002; Şen, 2008), where short, intense rains generate flash floods, whose water can be stored by shaping the wadi stream bed into a series of levelled terraces supported by spaced dikes. These terraces slow the water flow and increase infiltration (Oweis & Hachum, 1996; Oweis et al., 2001).

On the other hand, due to the sedimentation processes as a result of repeated surface runoff in the Wadi El Agarma sub-catchment and the absence of regular maintenance processes for these dikes, they lose their effect on harvesting and collecting runoff water behind the levelled terraces. On the 1st of March 2023, maintenance processes were carried out for six main dikes (Figure 29), one in the mainstream of El Agarma and 5 dikes in the secondary tributary of El Agarma (Olive tributary). As a result of the maintenance process, 13300 m^2 of levelled terraces were protected from degradation due to the lack of required water for olive and fig trees.

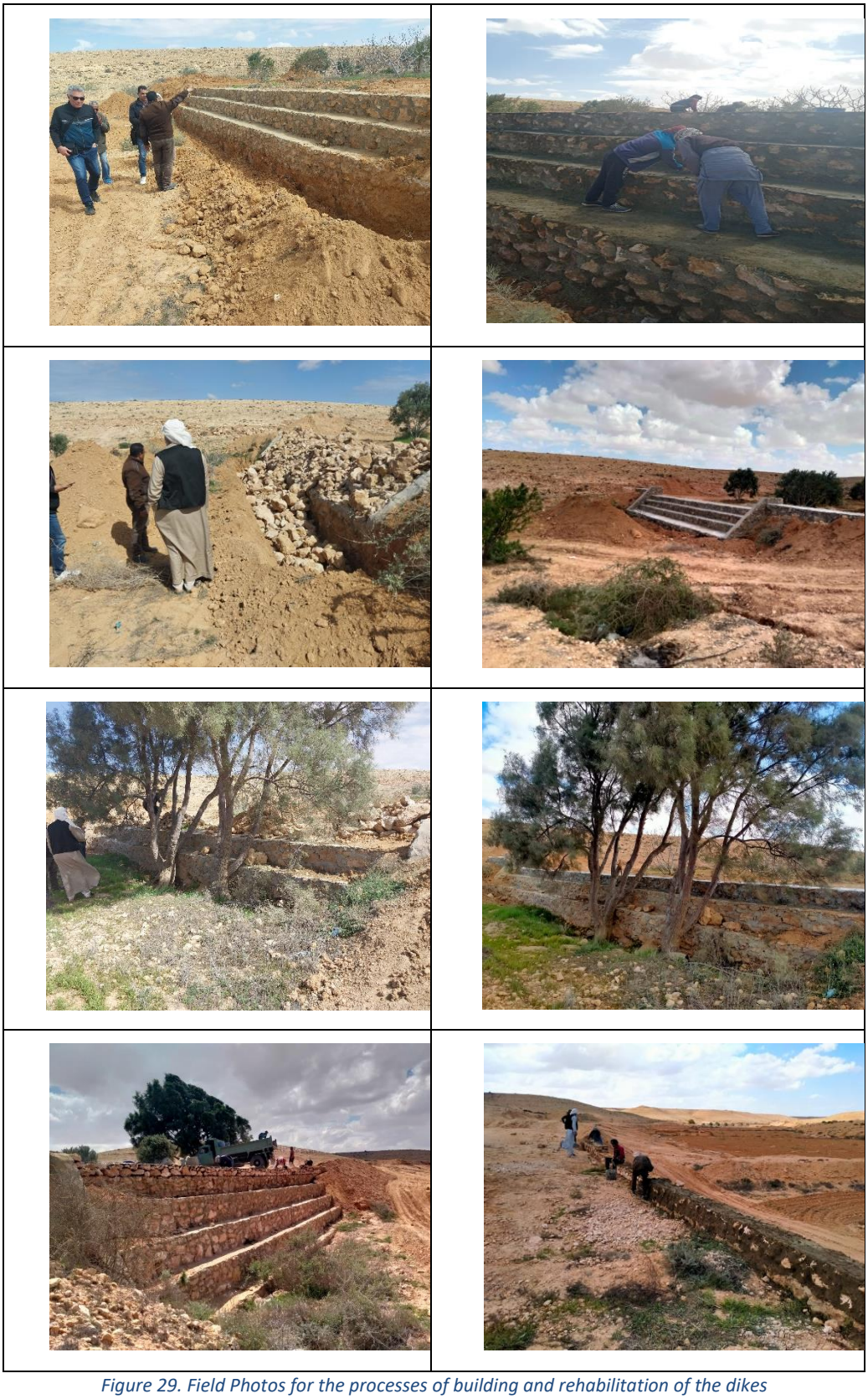

Figure 29. Field Photos for the processes of building and rehabilitation of the dikes

On 24 April 2023, after the maintenance processes had finished and a light shower of rainfall took place at Wadi El Agarma and the tributary that witnessed the maintenance processes, harvested considerable quantities of surface runoff (Figure 30) after a long period of drought due to the

ineffectiveness of the dikes before the rehabilitation process. We realized that rehabilitation and maintenance processes were effective.

Figure 30. Field photos of the harvested rainwater from the surface runoff after the maintenance process

3.2.2. Experimental design

Laboratory Soil Moisture Content measurements:

The setup for measuring moisture content in a laboratory involved the following steps:

- ❑ Choosing representative areas for sampling;
- ❑ Collecting soil samples at multiple locations within the sampling areas using a soil auger corer;
- ❑ Placing the samples in a drying oven at 104°C for 24 hours to dry the soil sample;
- ❑ After drying, weighing the samples to determine their dry weight and calculate the moisture content;
- ❑ Recording the results and labelling the samples for future measurements.

3.2.3. Soil Moisture Content Using Geophysical Techniques

Experimental Setup for Electrical Resistivity Tomography (ERT)

Electrical resistivity measurements of the soil along a surface transect are an alternative method to obtain information on sub-surface conditions, soil moisture content, and moisture dynamics [Brunet et al.2010; Daily et al., 2005; Friedman, 2005; and Samouëlian et al., 2005]. The method does not require coring, has minimal disturbance to the soil body (non-destructive measurement method), yields information to a depth of several meters, and is repeatable. If the assumption is made that the resistivity effects of structural soil properties remain constant through time, then differences in resistivity between repeat measurements may be attributed to changes in soil moisture content. Regular measurements of soil electrical resistivity during the growing season and after precipitation events can therefore yield important information on moisture availability and vegetation water use over time.

The setup for measuring moisture content in the field using electrical resistivity imaging typically involves the following steps (Figure 31):

- ❑ Selection of a suitable location for the measurement, so that the site is representative of the area of interest (aoi) before the terraces dam. The ERT measuring period (summer and winter) provides insight into soil moisture dynamics. Samples will be taken at the beginning, middle, and at end of the period.
- ❑ ERT data will be collected using the SYSCAL JUNIOR advanced resistivity meter with a Wenner configuration with 0.25 and 1 m spacing over a transect length of 8.75 and 35 respectively m, which provides reliable resistivity information to a depth of approximately 1m for SWC and 9.5 m for detect depth to bed rock for the largest electrode spacing within the total line and provides the best trade-off between horizontal and vertical resolution.
- ❑ Apply a current to the electrodes and the voltage difference between different electrodes to determine the electrical resistivity of the subsurface materials.
- ❑ Collect data at multiple locations across the site to create a conductive profile or map of the resistivity distribution.
- ❑ Process the collected data using RES2Dinv (ver.4.08) (www.getomosof.com) software to generate a 2D image of the subsurface conductivity/resistivity distribution.
- ❑ Interpret the resistivity/conductivity images to identify areas of high or low conductivity in the subsurface.
- ❑ Validate the results by comparing them with the nearest measured SWC or ground truth data.

It is essential to calibrate the resistivity equipment and follow standardized procedures to ensure accurate and reliable measurements of content in the field using electrical resistivity imaging.

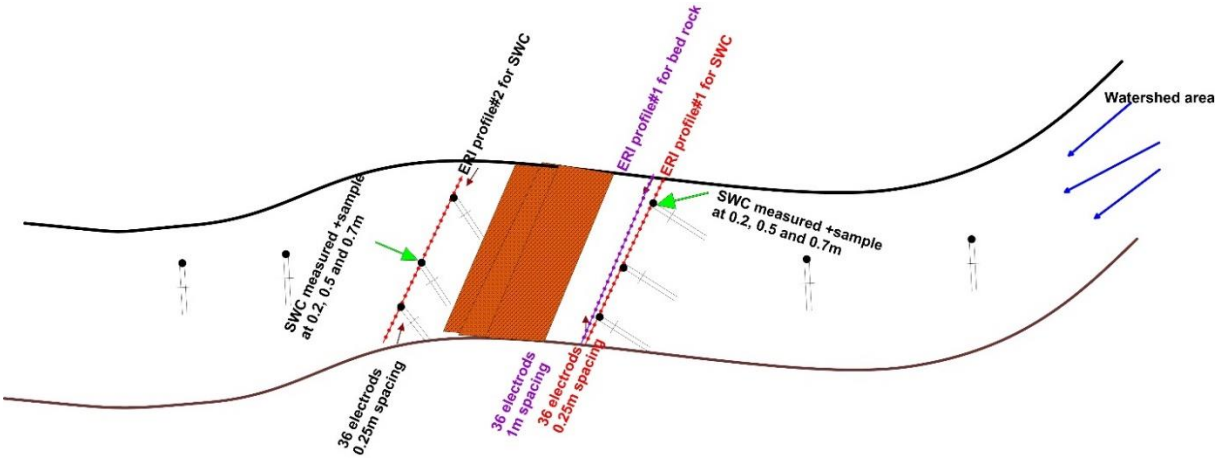

Figure 31. A simplified conceptual model for the Experimental design in living lab to obtain soil water content (SWC)

3.3. Results

3.3.1. Soil Physical Properties

Soil Particle Size Distribution and Textural Class

The range and proportion of different-sized particles within soil are referred to as the “particle size distribution” or sometimes “mechanical analysis,” which involves separating soil into its various size

categories: gravel, sand, silt, and clay. This distribution plays a crucial role in determining how soil behaves in different uses. Since soil is composed of mineral particles, both their size and arrangement significantly affect its properties. Within a single soil sample, particle sizes can vary widely—from very coarse particles larger than 100 mm to extremely fine ones smaller than 2 microns.

At the El-Safa site, the information presented in Table 2 and Figure 32 indicates that the surface layers of the soil profiles mostly exhibit a texture ranging from loamy sand to sandy loam. When comparing particle size distribution across the surface layers at this site, it becomes clear that there is a relatively high content of both coarse and fine sand, accompanied by a comparatively lower proportion of silt and clay. This pattern is especially noticeable in the surface layers of El-Safa sites (4) and (5).

Table 2 . Particle size distribution and textural class of the El-Safa selected soil surface layer.

Soil sample NO.	Particle size distribution (%)					Textural class
	Coarse Sand %	Fine Sand %	Total Sand	Silt	Clay	
El Safa (1)	18.97	45.10	64.07	17.01	18.91	Sandy Loam
El Safa (2)	19.71	38.79	58.50	24.90	16.60	Sandy Loam
El Safa (3)	17.06	46.29	63.35	19.42	17.22	Sandy Loam
El Safa (4)	70.52	12.38	82.90	9.09	8.01	Loamy Sand
El Safa (5)	47.28	37.58	84.83	12.64	2.53	Loamy Sand

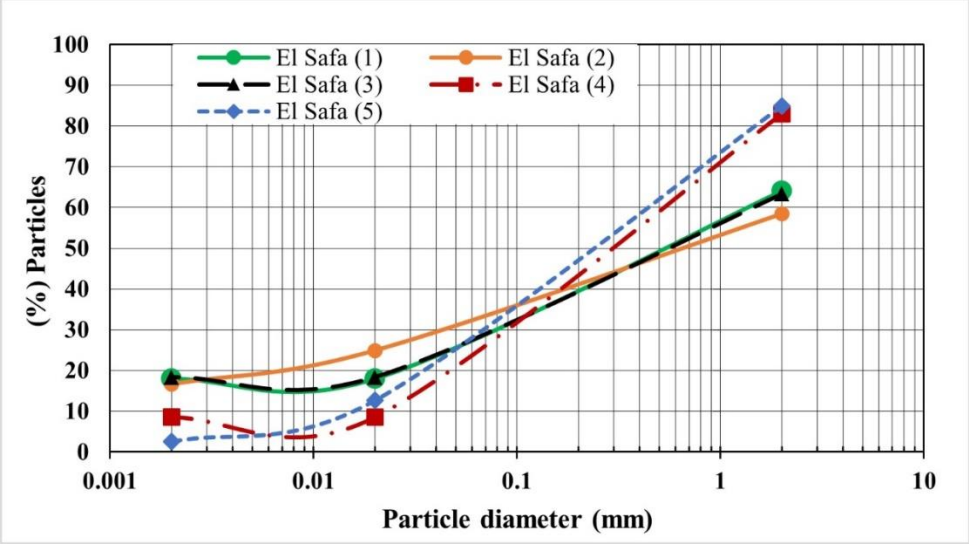

Figure 32. particle size distribution of the El-Safa selected soil surface layer

For the El-Raml site, the soil particle size fractions across the examined depths are provided in Table 3 and illustrated in Figure 33. The data show that the total sand content in the various surface soil layers ranges between 71.02% and 85.08%, while the clay content varies from 4.85% to 14.32%. These values indicate that the soil texture in the surface layers generally falls within the loamy sand to sandy loam categories.

Table 3. Particle size distribution and textural class of the El Raml selected soil surface layer.

Soil sample NO.	Particle size distribution (%)					Textural class
	Coarse Sand %	Fine Sand %	Total Sand	Silt	Clay	
El Raml (1)	21.47	59.13	80.59	14.55	4.85	Loamy Sand
El Raml (2)	8.52	63.09	71.61	18.93	9.46	Sandy Loam
El Raml (3)	34.18	50.90	85.08	9.94	4.97	Loamy Sand
El Raml (4)	15.10	55.92	71.02	9.66	19.32	Sandy Loam
El Raml (5)	19.61	58.60	78.21	16.34	5.45	Loamy Sand
El Raml (6)	17.04	57.52	74.56	20.35	5.09	Sandy Loam

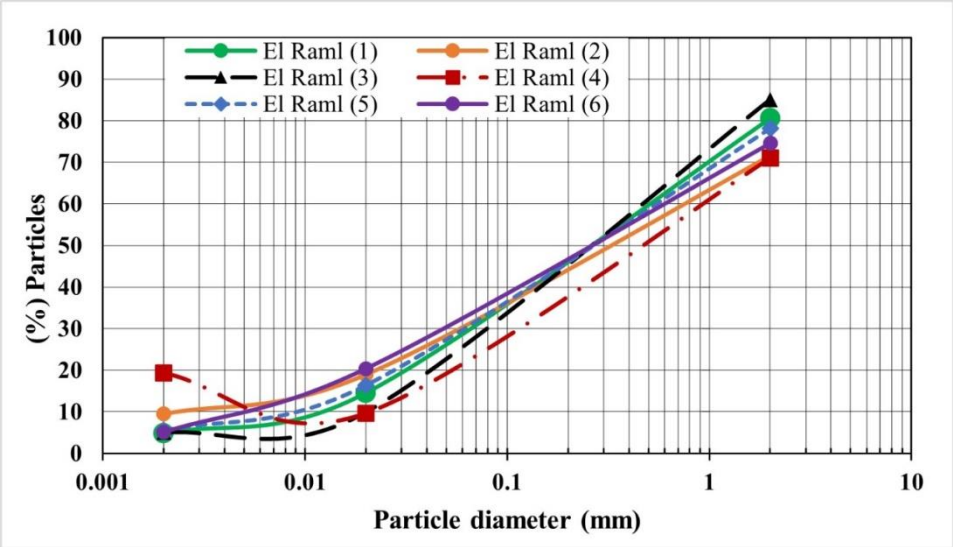

Figure 33. Particle size distribution of El Raml selected soil surface layer

Considering Al-Agarma site, data given in Table 4 and Figure 34 elucidate that most of the studied soils in such an area are characterized by sandy loam texture.

Table 4. Particle size distribution and textural class of the El Agharma selected soil surface layer

Soil sample NO.	Particle size distribution (%)					Textural class
	Coarse Sand %	Fine Sand %	Total Sand	Silt	Clay	
Al Agharma (1)	5.78	68.03	73.82	12.10	14.08	Sandy Loam
Al Agharma (2)	17.28	60.12	77.41	13.56	9.04	Sandy Loam
Al Agharma (3)	16.89	53.55	70.44	21.11	8.45	Sandy Loam
Al Agharma (4)	20.78	55.75	76.52	14.09	9.39	Sandy Loam
Al Agharma (5)	23.47	53.85	77.32	13.61	9.07	Sandy Loam
Al Agharma (6)	9.36	68.61	77.97	17.62	4.41	Loamy Sand

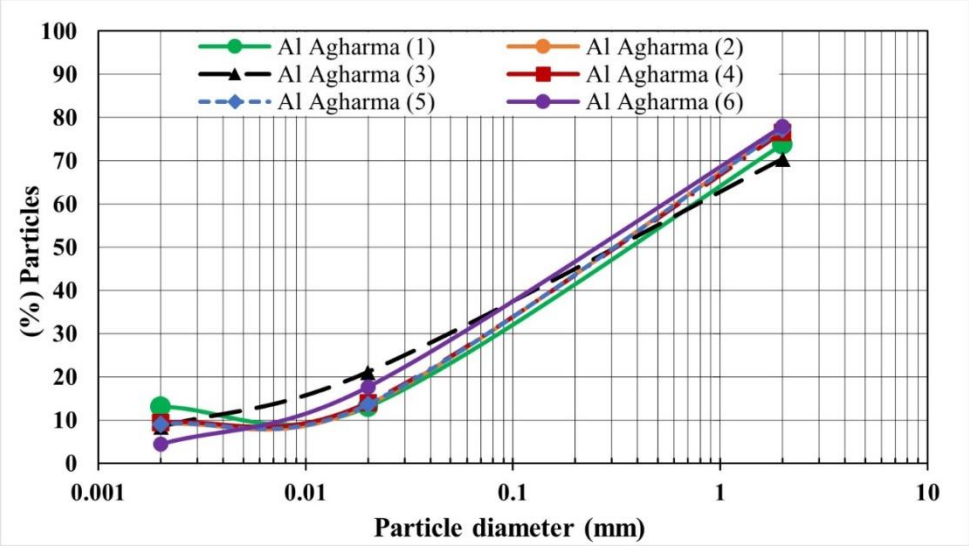

Figure 34. particle size distribution of the El Agharma selected soil surface layer

3.3.2. Soil Moisture Profile Distribution

Soil moisture serves as a vital connection between rainfall, surface water, and groundwater, and it varies across both space and time due to several hydrological processes such as infiltration, runoff, wind and freeze-thaw erosion, and the movement of sediments and pollutants. In arid and water-limited regions, soil moisture is especially critical for plant growth, the development of ecological systems, and the recovery of degraded vegetation. The way soil moisture responds to precipitation is a key part of the water cycle—this relationship has gained increasing importance amid global climate change, which has led to more erratic rainfall patterns. As a result, researchers around the world are paying closer attention to how precipitation affects soil moisture in dry environments. Gaining insight into this relationship is essential for managing scarce water resources effectively.

Vertically, soil moisture is affected by both intrinsic soil characteristics (like texture and bulk density) and external environmental conditions (such as rainfall, evaporation, and land use patterns).

At the El Kharoopa Valley site, data presented in Table 5 and shown in Figure 35 indicate that the soil moisture levels in the second profile are noticeably higher than those in the first. Additionally, moisture content increases progressively with soil depth in both profiles

Table5 . Soil moisture content (%) of different soil profile layers of the El Kharoopa Valley study area

Profile No. (El Kharoopa Valley Study area)	Depth (cm)	Moisture Content (%)	Total porosity (%)
1	0-20	1.60	42.82
1	20-45	3.30	46.16
1	45-60	5.95	46.91
1	60-80+	5.79	44.22
2	0-20	4.19	47.82
2	20-45	4.97	43.78
2	45-60	6.33	42.30
2	60-80	7.91	44.26

2	80-100	8.97	43.72
2	100-120	9.91	45.49

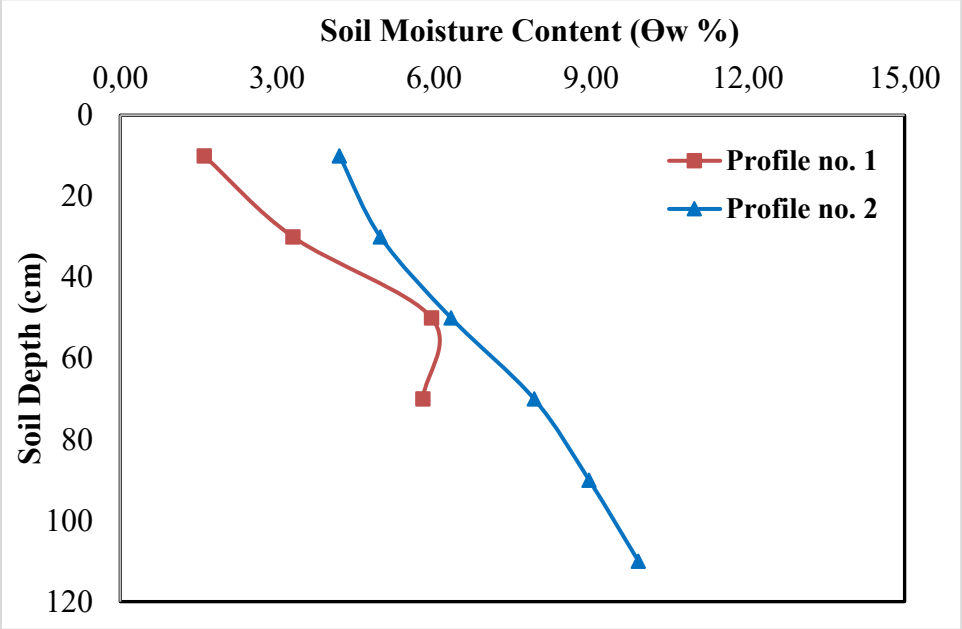

Figure 35. Soil moisture content (%) of different soil profile layers of El Kharoopa Vally study area

Regarding El-Raml site, the obtained values of soil moisture content of the studied soil profile depths are presented in Table 6 and shown in Figure 36. From these data it is evident that the soil moisture content of different sandy soil profile layers under investigation ranged from 1.81 to 6.63% for the profile 3 and varies from varies from 1.63% to 7.20% for the profile 4.

Table6 . Soil moisture content (%) of different soil profile layers of El Raml Valley study area

Profile NO. (El Ramel Valley study area)	Depth (cm)	Moisture Content (%)	Total porosity (%)
3	0-15	1.81	36.98
3	15-30	5.52	44.18
3	30-50	6.63	45.54
3	50-80	3.64	39.67
3	80-100	4.85	40.25
3	100-120	6.59	43.78
4	0-10	1.63	39.44
4	10-50	6.86	40.42
4	50-80	6.91	37.45
4	80-100	7.20	37.60
4	100-120	6.24	40.38

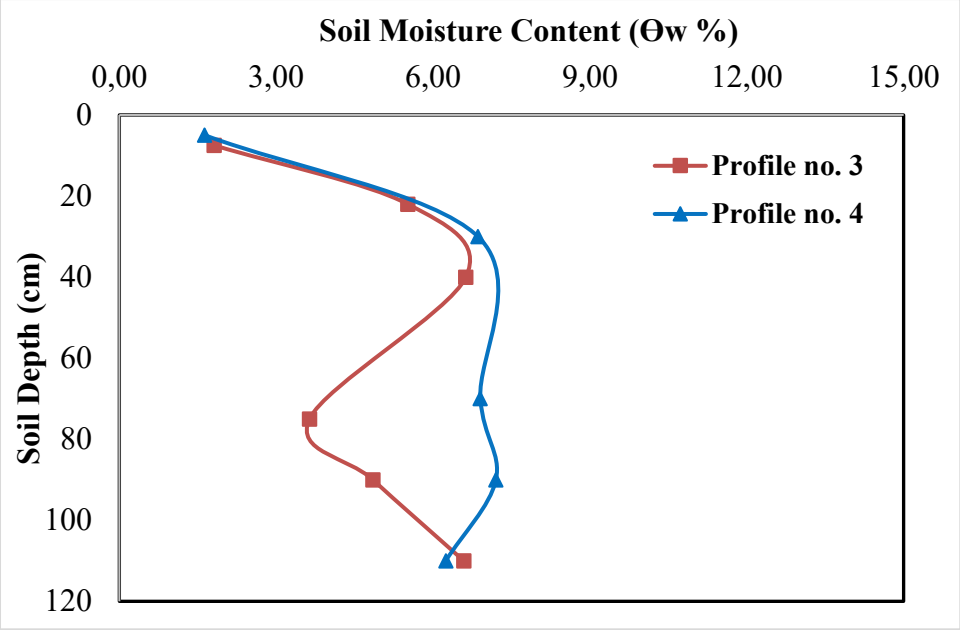

Figure 36. Soil moisture content (%) of different soil profile layers of El Ramel Vally study area

Considering Raghapet El Aghara, El Ramel Valley study area, data given in Table 7 and Figure 37 show the highest value of moisture content (6.01%), recorded at the fourth layer of the profile 6.

Table 7. Soil moisture content (%) of different soil profile layers of Raghapet El Aghara, El Ramel Valley study area.

Profile NO .(El Ramel Valley study area)	Depth (cm)	Moisture Content (%)	Total porosity (%)
5	0-15	1.54	43.79
5	15-50	2.58	32.26
5	50-90	3.48	36.88
5	90-110	3.25	36.16
6	0-15	0.77	32.00
6	15-45	1.89	36.67
6	45-70	5.29	40.94
6	70-110	6.01	40.89

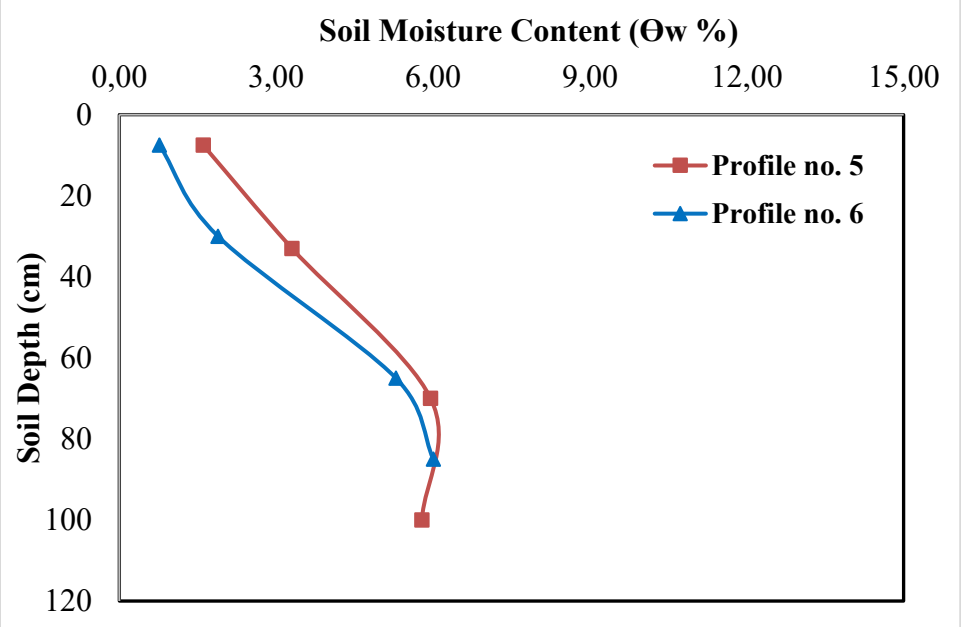

Figure 37. Soil moisture content (%) of different soil profile layers of Raghapet El Aghara, El Ramel Valley study area

3.3.3. Soil Infiltration Rate

Soil infiltration rate was measured by using the double-ring method. The Kostiakov model was used for interpreting the data collected in the monitoring sites. Kostiakov model is an empirical approach used to describe the infiltration of water into soils over time. It's widely used in hydrology, irrigation engineering, and soil science due to its simplicity and practical applicability.

In its basic form, it may be exp

The basic Kostiakov infiltration equation is:

$$i(t) = kt^{bn}$$

where:

$i(t)$: Infiltration rate at time t[L/T]

t: Time since the start of infiltration [T]

k, n: Empirical parameters

$k > 0$: initial infiltration capacity

$0 < n < 1$: controls the rate of decrease over time

In general, infiltration rate decreases over time, which matches observed behaviour in most soils.

The model assumes that infiltration will eventually approach zero, which is not realistic over long time periods.

The total depth of water infiltrated, I, up to time t may be obtained by integrating the previous equation for the infiltration rate

$$I(t) = \frac{k}{n+1} t^{n+1}$$

Results of Infiltration Rate in Watersheds

Infiltration rates were determined in different sites of the study area by using a double-ring infiltrometer method. The obtained results are shown in Figure 38. The results of the infiltration rate have been used as inputs in hydrological models.

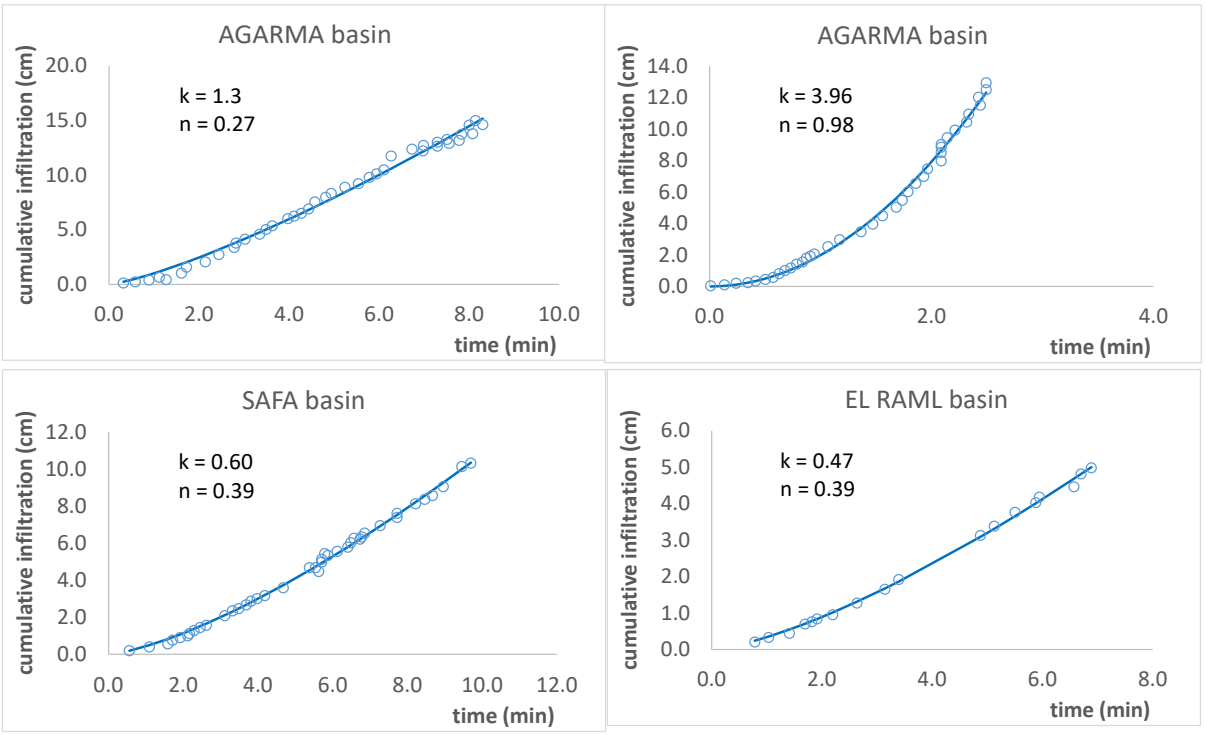

Figure 38. Infiltration rate results in the study area: a) Wadi Kharouba (Agarma and Safa sub-catchment, and b) Wadi ElRaml

3.3.4. Geophysical Measurements:

As geophysical methods provide fast, nondestructive tools to help understand soil heterogeneity by identifying spatial patterns of petrophysical parameters and relating them to hydrological properties or states, a multidimensional survey was conducted to improve our ability to understand the subsurface environmental fabric and observe its fluid dynamics that occur within it.

The applied survey was performed using automatic measurements of Electrical Resistivity Tomography (ERT) in parallel with traditional soil moisture measurements.

ERT data were collected using the SYSCAL JUNIOR advanced resistivity meter with a Wenner configuration with 0.25 m spacing over a transect length of 8.75 m, which provides reliable resistivity information to a depth of approximately 1 m for SW SWC and provides the best trade-off between horizontal and vertical resolution. Collected data were processed using RES2Dinv (ver.4.08) (www.getomosof.com) software to generate a 2D image of the subsurface conductivity/resistivity distribution of the resistivity/conductivity images to identify areas of high or low conductivity in the subsurface.

A key challenge in the fields of geophysics, petrophysics, and hydrology is assessing the volumetric water content or hydrocarbon saturation within porous subsurface materials based on geophysical measurements. Electrical resistivity techniques are among the most effective methods for this task, as the movement of electrical current through Earth materials mainly occurs through electrolytic processes and is thus highly responsive to the presence and chemistry of fluids in the pores. Archie's Law (Archie, 1942) serves as the foundational empirical relationship linking the bulk electrical resistivity of a clean, porous rock to its porosity and the resistivity of the fluid in the pores. This law continues to be essential for interpreting resistivity logs in oil and gas exploration, and its applications are expanding in hydrogeophysics and environmental research.

On the other hand, Archie's Law consists of a series of empirical relationships derived from experimental investigations of clean sandstone core samples. It indicates that the bulk electrical resistivity of a fully water-saturated rock (R_0) is directly proportional to the resistivity of the pore water (R_w) and inversely proportional to the porosity (phi).

The basic form of Archie's Law for a fully saturated formation is:

$$R0=a\cdot Rw\cdot\phi-m.R0=a\cdot Rw\cdot\phi^{-m}$$

Where R_0 is the bulk resistivity of the fully water-saturated rock (in Ω·m), R_w is the resistivity of the pore water (in Ω·m), phi is the porosity (unitless, fraction of total volume), a is the tortuosity factor (a constant, often near 1); and m is the cementation exponent (a constant that depends on the pore geometry and cementation, typically between 1.8 and 2.2 for sandstones).

The Formation Factor (F) simplifies this relationship:

$$F = R_o / R\_w = a \cdot \phi^{-m}$$

For partially saturated conditions:

$$R\_t = a \cdot R\_w \cdot \phi^{-m} \cdot S\_w^{-n}$$

where: R_t is the bulk resistivity of partially saturated rock, S_w is water saturation; and n is the saturation exponent.

Archie's Law plays a vital role in various fields of geoscience, such as hydrogeophysics for estimating soil moisture, environmental research for identifying contaminant plumes, and petroleum engineering for evaluating hydrocarbon saturation.

As illustrated in Figures 39 - 44, using both ERT and laboratory-measured SMC, Archie's Law has been applied to calculate the Soil Moisture Content at 6 basins.

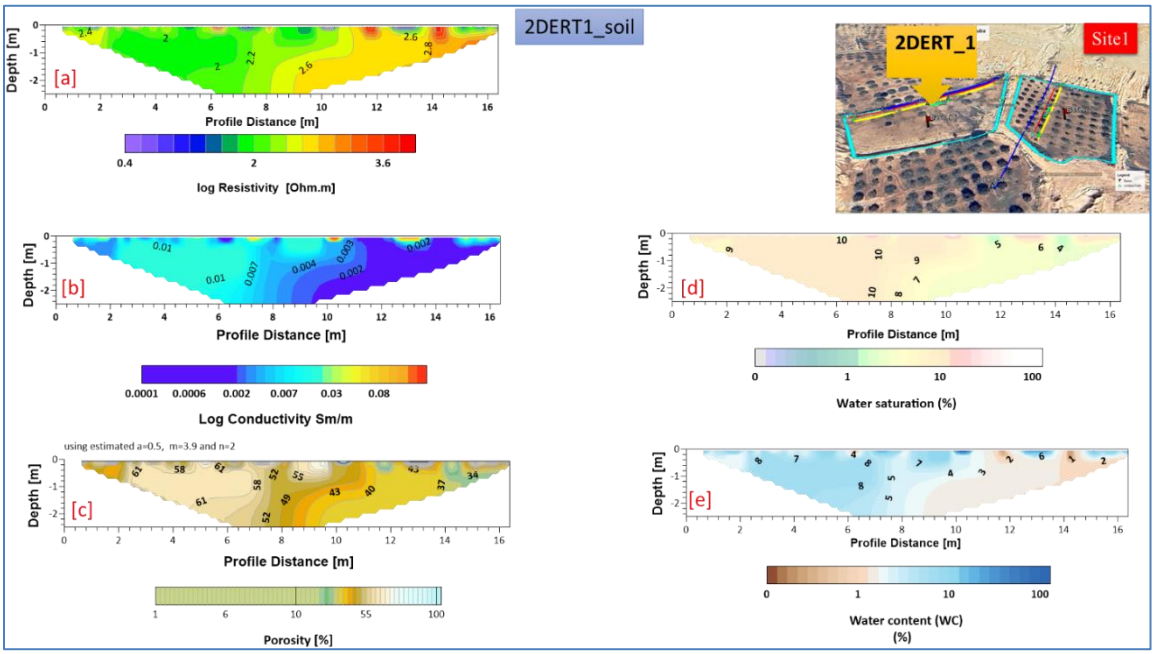

Figure 39. [a] log resistivity profile 1 at Basin 1 , [b] the distribution of subsurface conductivity of the soil in sm/m, [c] the distribution of soil porosity in %, [d] the distribution of water saturation of 2DERT1 and [e] the estimated water content or moisture content of subsurface soil in %.

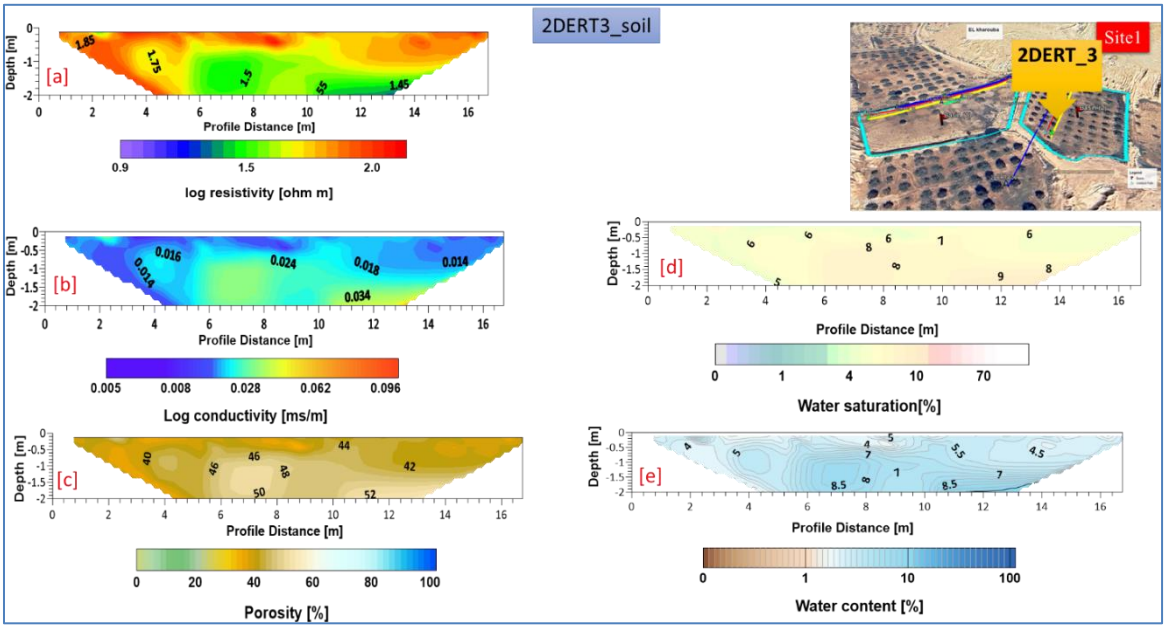

Figure 40. [a] log resistivity profile 3 at Basin 1, [b] the distribution of subsurface conductivity of the soil in sm/m, [c] the distribution of soil porosity in %, [d] the distribution of water saturation of 2DERT3, and [e] the estimated water content or moisture content of subsurface soil in %.

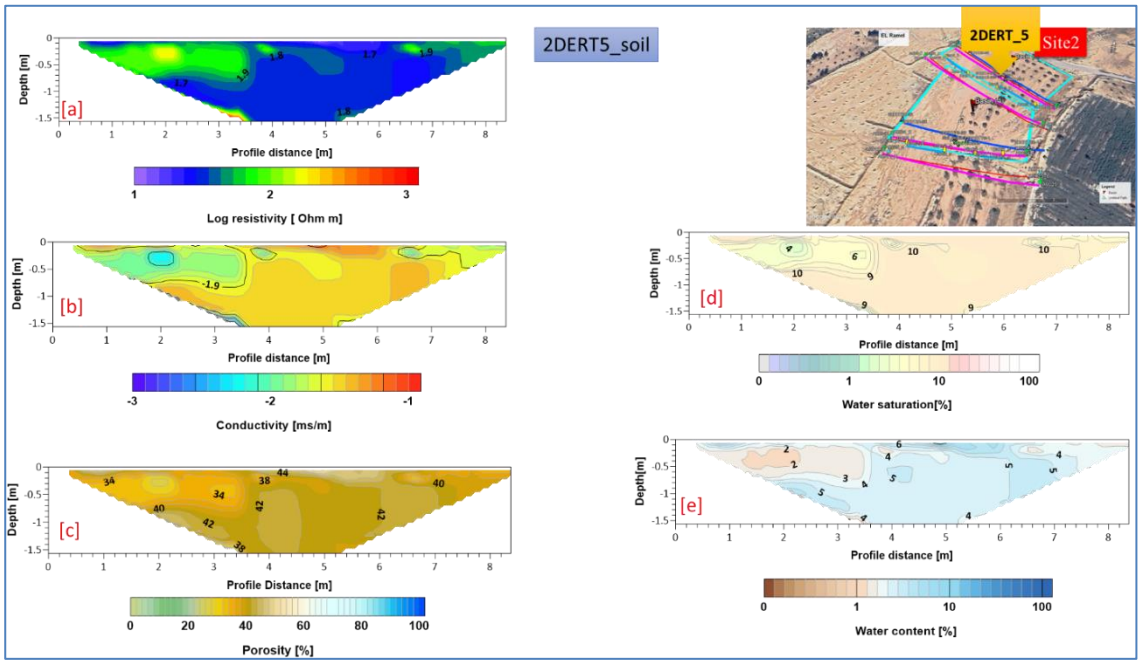

Figure 41. [a] log resistivity profile 5 at Basin 2 , [b] the distribution of subsurface conductivity of the soil in sm/m, [c] the distribution of soil porosity in %, [d] the distribution of water saturation of 2DERT5, and [e] the estimated water content or moisture content of subsurface soil in %.

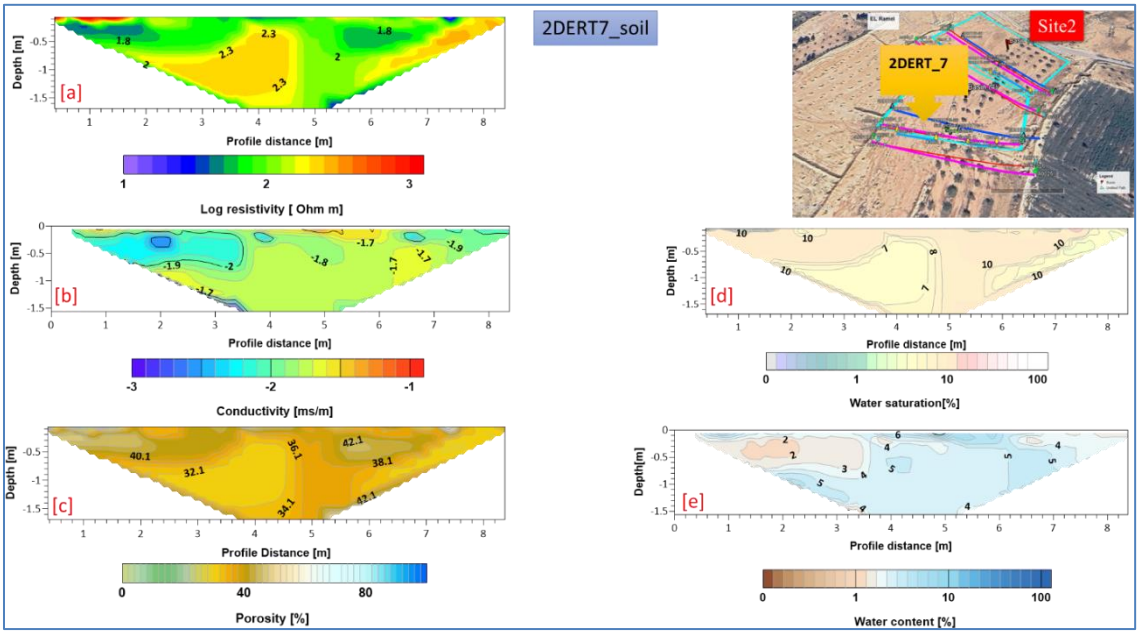

Figure 42. [a] log resistivity profile 7 at Basin 2, [b] the distribution of subsurface conductivity of the soil in sm/m, [c] the distribution of soil porosity in %, [d] the distribution of water saturation of 2DERT7, and [e] the estimated water content or moisture content of subsurface soil in %.

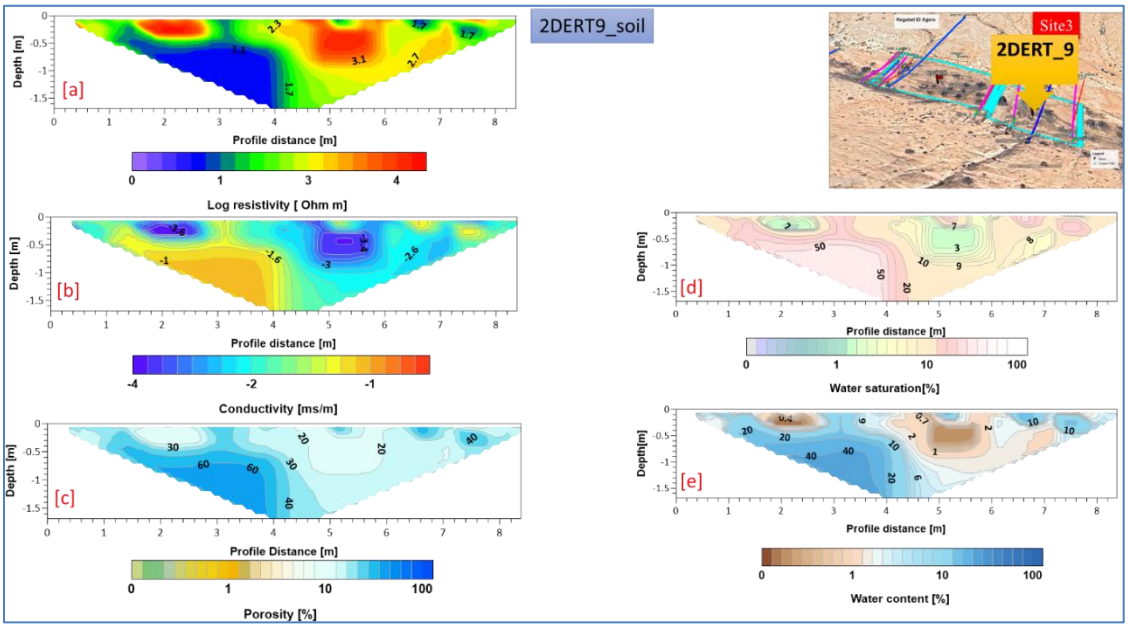

Figure 43. [a] log resistivity profile 9 at Basin 3, [b] the distribution of subsurface conductivity of the soil in sm/m, [c] the distribution of soil porosity in %, [d] the distribution of water saturation of 2DERT9, and [e] the estimated water content or moisture content of subsurface soil in %.

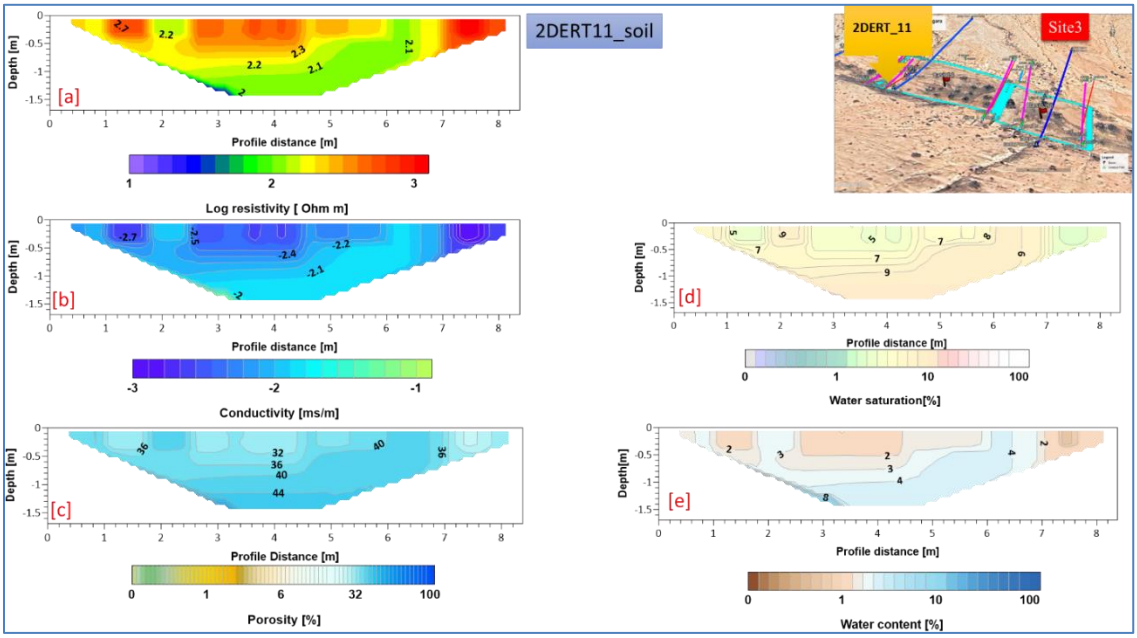

Figure 44. [a] log resistivity profile 11 at Basin 3, [b] the distribution of subsurface conductivity of the soil in sm/m, [c] the distribution of soil porosity in %, [d] the distribution of water saturation of 2DERT11, and [e] the estimated water content or moisture content of subsurface soil in %.

3.4. Discussion

The results of this research indicate a notable increase in soil moisture content (SMC) as depth increases, with values ranging from 1.5% to 9.9% throughout the sampled profile. While these laboratory measurements are accurate and essential for validation, they are somewhat limited: each sample represents merely a small, discrete location, providing a narrow and invasive glimpse into subsurface conditions. The true advantage of this study lies in the integration of these traditional measurements with Electrical Resistivity Tomography (ERT). As illustrated in Figure 5, the ERT survey delivered a continuous, high-resolution, two-dimensional depiction of the subsurface along the SMC column. This method not only delineated the various soil layers but also captured their changing characteristics with depth—something that drilling and sampling methods alone cannot achieve as efficiently or comprehensively. Notably, ERT was particularly effective in highlighting spatial differences in soil water content. By leveraging the inverse relationship between resistivity and moisture, it became possible to map areas of higher and lower water storage throughout the section. The alignment between the geophysical findings and the laboratory-measured SMC values enhances confidence in the approach. When combined, the incorporation of ERT with soil sampling illustrates how geophysics can transcend isolated data points, offering a more extensive framework that reveals both lateral continuity and subsurface variability. This, in turn, provides a clearer understanding of how water moves, accumulates, and is retained underground—critical insights for managing subsurface hydrology.

3.5. Implications for policymakers

- Evidence-driven decision-making: Integrated geophysical monitoring delivers trustworthy data regarding groundwater, soil health, and land degradation, facilitating focused efforts to combat desertification.
- Water security approaches: Findings underscore the importance of merging water harvesting, aquifer storage management, and geophysical studies to secure additional groundwater resources in arid regions.
- Sustainable farming: The implementation of soil-water conservation methods, guided by geophysical knowledge, boosts crop resilience amidst climate challenges.
- Capacity enhancement: Investments in local skill development and technology sharing are essential to bolster national capabilities in the fight against desertification.
- Policy alignment: Results support the incorporation of geophysical methods into national initiatives for desertification management, ensuring consistency with climate adaptation and sustainable development objectives.

3.6. Conclusion

This study emphasizes the importance of combining geophysical techniques with conventional soil research. Specifically, Electrical Resistivity Tomography (ERT) has emerged as a formidable method that transforms our understanding of soil-water relationships. The ERT profiles successfully differentiated various soil types and accurately pinpointed zones with differing moisture levels. The strong correlation observed between geophysical analyses and lab results supports the idea that ERT can act as a reliable technique for quantitative hydrological evaluation.

One of the most significant advantages of this integrated method is its capacity to reconcile precision with scale. Although laboratory assessments are crucial for calibration and validating results, they are inherently restricted in their geographic reach. ERT addresses this limitation by providing spatial continuity and revealing the variability and interconnections of subsurface layers that influence water behavior.

For future work, the consistent application of ERT—alongside other complementary technologies like Ground Penetrating Radar (GPR)—should be adopted as standard methodology. When adjusted with local soil moisture data, these methods can yield precise, scalable insights into water distribution. This advancement will not only enhance our scientific knowledge but also offer practical advantages for managing water resources, agriculture, and long-term planning in areas facing water scarcity.

4. References

El Amami, S. 1984. Les aménagements hydrauliques traditionnels en Tunisie. Centre de recherche en Génie Rural (CRGR). Tunis, 69 pp.

El Amami, S. 1982. The traditional hydraulic structures in the Maghreb (in Arabic). ACSAD, Damascus, Syria. 35 pp + Annexes.

Alaya, K., Viertmann, W., Waibel, Th. 1993. Les tabias. Imprimerie Arabe de Tunisie,Tunis, Tunisia. 192 pp.

Andrino, A., Guggenberger, G., Kernchen, S., Mikutta, R., Sauheitl, L., & Boy, J. (2021). Production of Organic Acids by Arbuscular Mycorrhizal Fungi and Their Contribution in the Mobilization of Phosphorus Bound to Iron Oxides. Frontiers in Plant Science, 12. https://www.frontiersin.org/journals/plant-science/articles/10.3389/fpls.2021.661842

Aoda, M. I., Smucker, A. J. M., Majeed, S. S., Mohammed, H. A., Al-Sahaf, F. H., & Robertson, G. P. (2021). Novel root zone soil water retention improves production with half the water in arid sands. Agronomy Journal, 113(3), 2398–2406. https://doi.org/10.1002/agj2.20648

Archie, G. E. (1942). The electrical resistivity log as an aid in determining some reservoir characteristics. Transactions of the AIME, 146(1), 54-62.

Arnon, D. I. (1949). Copper Enzymes in Isolated Chloroplasts. Polyphenoloxidase in Beta Vulgaris. Plant Physiology, 24(1), 1–15. https://doi.org/10.1104/pp.24.1.1

Aubert, G. (1978). Méthodes d'analyses des sols. 2ème Edition. Centre Régional de Documentation Pédagogique, CRDP Marseille, 191 p.

Bahadur, A., Batool, A., Nasir, F., Jiang, S., Mingsen, Q., Zhang, Q., Pan, J., Liu, Y., & Feng, H. (2019). Mechanistic insights into arbuscular mycorrhizal fungi-mediated drought stress tolerance in plants. International Journal of Molecular Sciences, 20(17), 1–18. https://doi.org/10.3390/ijms20174199

Baker, N. R. (2008). Chlorophyll fluorescence: A probe of photosynthesis in vivo. Annual Review of Plant Biology, 59, 89–113. https://doi.org/10.1146/annurev.arplant.59.032607.092759

Baslam, M., Mitsui, T., Hodges, M., Priesack, E., Herritt, M. T., Aranjuelo, I., & Sanz-Sáez, Á. (2020). Photosynthesis in a Changing Global Climate: Scaling Up and Scaling Down in Crops. Frontiers in Plant Science, 11(July), 1–29. https://doi.org/10.3389/fpls.2020.00882

Begum, N., Qin, C., Ahanger, M. A., Raza, S., Khan, M. I., Ashraf, M., Ahmed, N., & Zhang, L. (2019). Role of Arbuscular Mycorrhizal Fungi in Plant Growth Regulation: Implications in Abiotic Stress Tolerance. Frontiers in Plant Science, 10(September), 1–15. https://doi.org/10.3389/fpls.2019.01068

Belayneh, M., Yirgu, T., & Tsegaye, D. (2019). Effects of soil and water conservation practices on soil physicochemical properties in Gumara watershed, Upper Blue Nile Basin, Ethiopia. Ecological Processes, 8(1). https://doi.org/10.1186/s13717-019-0188-2

Ben Mechlia, N. and Ouessar, M.: Water harvesting systems in Tunisia, in: Indigenous water harvesting in West Asia and North Africa, edited by: Oweis, T., Hachum, A., and Bruggeman, A., ICARDA, Aleppo, Syria, 21–41, 2004.

Binley A., Hubbard S.S., Huisman J.A., Revil A., Robinson D.A., Singha K., & Slater L.D. (2015). The emergence of hydrogeophysics for improved understanding of subsurface processes over multiple scales. Water Resources Research, 51(6), 3837–3866. https://doi.org/10.1002/2015WR017016

Boutasknit, A., Ait-el-mokhtar, M., Fassih, B., & Ben-laouane, R. (2024). Effect of Arbuscular Mycorrhizal Fungi and Rock Phosphate on Growth , Physiology , and Biochemistry of Carob under Water Stress and after Rehydration in Vermicompost-Amended Soil.

Boutasknit, A., Baslam, M., Ait-El-Mokhtar, M., Anli, M., Ben-Laouane, R., Ait-Rahou, Y., Mitsui, T., Douira, A., El Modafar, C., Wahbi, S., & Meddich, A. (2021). Assemblage of indigenous arbuscular mycorrhizal fungi and green waste compost enhance drought stress tolerance in carob (Ceratonia siliqua L.) trees. Scientific Reports, 11(1), 1–23. https://doi.org/10.1038/s41598-021-02018-3

BRADFORD, M. M. (1976). A Rapid and Sensitive Method for the Quantitation Microgram Quantities of Protein Utilizing the Principle of Protein-Dye Binding. Analytical Biochemistry, 7(5), 248–254. https://doi.org/10.1016/0003-2697(76)90527-3

Bruggeman, A., van der Meijden, G. 2005. Assessment of water use in a small watershed in Northern Syria using SWAT. In: Srinivasan, R., Jennifer, J., Day, D., Abbaspour, K. (eds). Proceedings of the 3rd international SWAT conference, pp: 50-60.

Brunet P., Clément R., & Bouvier C. (2010). Monitoring soil water content and deficit using Electrical Resistivity Tomography (ERT) – A case study in the Cevennes area, France. Journal of Hydrology, 380(3–4), 146–153. https://doi.org/10.1016/j.jhydrol.2009.10.028

Chakhchar, A., Ben Salah, I., El Kharrassi, Y., Filali-Maltouf, A., El Modafar, C., & Lamaoui, M. (2022). Agro-Fruit-Forest Systems Based on Argan Tree in Morocco: A Review of Recent Results. Frontiers in Plant Science, 12(January). https://doi.org/10.3389/fpls.2021.783615

Daily W., Ramirez A., Binley A., & LaBrecque D. (2005). Electrical resistance tomography, theory and practice. In D.K. Butler (Ed.), Near-surface geophysics (pp. 525–550). Society of Exploration Geophysicists. https://doi.org/10.1190/1.9781560801719.ch17

Defaa, C., Elantry, S., Lahlimi, S., Alami, E., Achour, A., Mousadik, A. El, & Msanda, F. (2015). Effects of Tree Shelters on the Survival and Growth of Argania spinosa Seedlings in Mediterranean Arid

Environment. International Journal of Ecology, 2015, 6 pages. https://doi.org/http://dx.doi.org/10.1155/2015/124075

Del Buono, D. (2021). Can biostimulants be used to mitigate the effect of anthropogenic climate change on agriculture? It is time to respond. Science of the Total Environment, 751, 141763. https://doi.org/10.1016/j.scitotenv.2020.141763

Dragonetti G., Farzamian M., Basile A., Monteiro Santos F., & Coppola A. (2022). In situ estimation of soil hydraulic and hydrodispersive properties by inversion of electromagnetic induction measurements and soil hydrological modeling. Hydrology and Earth System Sciences, 26(19), 5119–5136. https://doi.org/10.5194/hess-26-5119-2022

Dubois, M., Gilles, K., Hamilton, J. K., Rebers, P. A., & Smith, F. (1956). A colorimetric method for the determination of sugars. Nature, 168(4265), 167. https://doi.org/https://doi.org/10.1021/ac60111a017

Dumanović, J., Nepovimova, E., Natić, M., Kuča, K., & Jaćević, V. (2021). The Significance of Reactive Oxygen Species and Antioxidant Defense System in Plants: A Concise Overview. Frontiers in Plant Science, 11(January). https://doi.org/10.3389/fpls.2020.552969

Fang, Y., & Xiong, L. (2015). General mechanisms of drought response and their application in drought resistance improvement in plants. Cellular and Molecular Life Sciences, 72(4), 673–689. https://doi.org/10.1007/s00018-014-1767-0

Figueiredo, A. F., Boy, J., & Guggenberger, G. (2021). Common Mycorrhizae Network: A Review of the Theories and Mechanisms Behind Underground Interactions. Frontiers in Fungal Biology, 2. https://www.frontiersin.org/journals/fungal-biology/articles/10.3389/ffunb.2021.735299

Floret, C., Pontanier, R. 1982. L'aridité en Tunisie présaharienne : Climat, sol, végétation et aménagement. ORSTOM, Paris.

Friedman S.P. (2005). Soil properties influencing apparent electrical conductivity: A review. Computers and Electronics in Agriculture, 46(1–3), 45–70. https://doi.org/10.1016/j.compag.2004.11.001

Gaubi E (1995) Synthèse hydrogéologique sur la nappe des Grès du Trias (Gouvernorats de Médenine et Tatouine). Rapport Interne. DGRE 44p.

Gauillard, F., Richardforget, F., & Nicolas, J. (1993). New Spectrophotometric Assay for Polyphenol Oxidase Activity. Analytical Biochemistry, 215(1), 59–65. https://doi.org/https://doi.org/10.1006/abio.1993.1554

Ghazali, H. El, Daoud, S., & Tlemçani, N. B. (2021). Impact of Climate Change on the Argan Biosphere Reserve (ABR) in Morocco. May. https://doi.org/10.20944/preprints202105.0536.v1

Glover, P. W. J. (2015). Geophysical properties of the near-surface Earth: Electrical properties. In G. Schubert (Ed.), Treatise on Geophysics (2nd ed., Vol. 11, pp. 89-137). Elsevier. https://doi.org/10.1016/B978-0-444-53802-4.00189-5

Guber, A. K., Smucker, A. J. M., Berhanu, S., & Miller, J. M. L. (2015). Subsurface Water Retention Technology Improves Root Zone Water Storage for Corn Production on Coarse-Textured Soils. Vadose Zone Journal, 14(7), 1–13. https://doi.org/10.2136/vzj2014.11.0166

Huisman J.A., Hubbard S.S., Redman J.D., & Annan A.P. (2003). Measuring soil water content with ground penetrating radar. Vadose Zone Journal, 2(4), 476–491. https://doi.org/10.2136/vzj2003.4760

Kapoor, R., Evelin, H., Mathur, P., & Giri, B. (2013). Arbuscular Mycorrhiza: Approaches for Abiotic Stress Tolerance in Crop Plants for Sustainable Agriculture. In Plant Acclimation to Environmental Stress. https://doi.org/10.1007/978-1-4614-5001-6

Kavdir, Y., Zhang, W., Basso, B., & Smucker, A. J. M. (2014). Development of a new long-term drought resilient soil water retention technology. Journal of Soil and Water Conservation, 69(5), 154A-160A. https://doi.org/10.2489/jswc.69.5.154A

Khaliq, A., Perveen, S., Alamer, K. H., Zia Ul Haq, M., Rafique, Z., Alsudays, I. M., Althobaiti, A. T., Saleh, M. A., Hussain, S., & Attia, H. (2022). Arbuscular Mycorrhizal Fungi Symbiosis to Enhance Plant–Soil Interaction. In Sustainability (Vol. 14, Issue 13). https://doi.org/10.3390/su14137840

Klenk P., Jaumann S., & Roth K. (2015). Quantitative high-resolution observations of soil water dynamics in a complicated architecture using time-lapse ground-penetrating radar. Hydrology and Earth System Sciences, 19(3), 1125–1139. https://doi.org/10.5194/hess-19-1125-2015

Lahbouki, S., Anli, M., El Gabardi, S., Ait-El-Mokhtar, M., Ben-Laouane, R., Boutasknit, A., Ait-Rahou, Y., Outzourhit, A., Wahbi, S., Douira, A., & Meddich, A. (2022). Evaluation of arbuscular mycorrhizal fungi and vermicompost supplementation on growth, phenolic content and antioxidant activity of prickly pear cactus (Opuntia ficus-indica). Plant Biosystems, 156(4), 882–892. https://doi.org/10.1080/11263504.2021.1947408

Lahbouki, S., Ech-Chatir, L., Er-Raki, S., Outzourhit, A., & Meddich, A. (2022). Improving drought tolerance of Opuntia ficus-indica under field using subsurface water retention technology: changes in physiological and biochemical parameters. Canadian Journal of Soil Science, 102(4), 888–898. https://doi.org/10.1139/cjss-2022-0022

Lahbouki, S., Meddich, A., Ben-laouane, R., & Outzourhit, A. (2022). Subsurface Water Retention Technology Promotes Drought Stress Tolerance in Field-Grown Tomato. Energies, 15, 6807.

Lefhaili, A. (2010). FAO Forest Resources Assessment: Morocco Country Report.

León-Sánchez, L., Nicolás, E., Prieto, I., Nortes, P., Maestre, F. T., & Querejeta, J. I. (2020). Altered leaf elemental composition with climate change is linked to reductions in photosynthesis, growth and survival in a semi-arid shrubland. Journal of Ecology, 108(1), 47–60. https://doi.org/10.1111/1365-2745.13259

Liu, Y., Zhang, G., Luo, X., Hou, E., Zheng, M., Zhang, L., He, X., Shen, W., & Wen, D. (2021). Mycorrhizal fungi and phosphatase involvement in rhizosphere phosphorus transformations improves plant nutrition during subtropical forest succession. Soil Biology and Biochemistry, 153(June 2020), 108099. https://doi.org/10.1016/j.soilbio.2020.108099

Loeffler O., & Bano M. (2004). Ground penetrating radar measurements in a controlled vadose zone. Vadose Zone Journal, 3(4), 1082–1092. https://doi.org/10.2136/vzj2004.1082

Lu Y., Song W., Lu J., Wang X., & Tan Y. (2017). An examination of soil moisture estimation using ground penetrating radar in desert steppe. Water, 9(7), 521. https://doi.org/10.3390/w9070521

Lunt I.A., Hubbard S.S., & Rubin Y. (2005). Soil moisture content estimation using ground-penetrating radar reflection data. Journal of Hydrology, 307(1–4), 254–269. https://doi.org/10.1016/j.jhydrol.2004.10.014

Luján Soto, R., Martínez-Mena, M., Cuéllar Padilla, M., & de Vente, J. (2021). Restoring soil quality of woody agroecosystems in Mediterranean drylands through regenerative agriculture. Agriculture, Ecosystems and Environment, 306(August 2020). https://doi.org/10.1016/j.agee.2020.107191

Naouraz, M., Chehab, H., Aissaoui, F., Dabbaghi, O., Attia, F., Mahjoub, Z., & Carotenoids, C. (2018). Effects of mycorrhizal fungi inoculation and soil amendment with hydrogel on leaf anatomy , growth and physiology performance of olive plantlets under two contrasting water regimes. Acta Physiologiae Plantarum, 0(0), 0. https://doi.org/10.1007/s11738-018-2692-x

Nkurunziza, L., Chirinda, N., Lana, M., Sommer, R., Karanja, S., Rao, I., Romero Sanchez, M. A., Quintero, M., Kuyah, S., Lewu, F., Joel, A., Nyamadzawo, G., & Smucker, A. (2019). The Potential Benefits and Trade-Offs of Using Sub-surface Water Retention Technology on Coarse-Textured Soils: Impacts of Water and Nutrient Saving on Maize Production and Soil Carbon Sequestration. Frontiers in Sustainable Food Systems, 3(September), 1–10. https://doi.org/10.3389/fsufs.2019.00071

Neffati, M. 1994. Caracterisation morpho-biologique de certaines especes végétales Nord Africaines : Implications pour l'amélioration pastorale. Ph.D. thesis, Ghent University, Belgium.

Olsen, S., & Sommers, L. (1982). Phosphorus. Methods of soil analyses, part 2. Chemical and microbiological properties. Agron Monogr, 9, 421–422.

Ouessar M. 2007. Hydrological impacts of rainwater harvesting in wadi Oum Zessar watershed (Southern Tunisia). Ph.D. thesis, Faculty of Bioscience Engineering, Ghent University, Ghent, Belgium, 154 pp.

Ouled Belgacem, A. 2006. Statut écologique performance biologique et aptitude à la réinstallation de Stipa lagascae dans les écosystèmes dégradés des milieux arides tunisiens. Ph.D. thesis, Faculté des Sciences de Sfax, Tunisia.

Oweis T., & Hachum A. (1996). Water harvesting and supplemental irrigation for improved water use efficiency in dry areas. International Water Management Institute (IWMI), SWIM Paper 7.

Oweis T., Prinz D., & Hachum A. (2001). Water harvesting: Indigenous knowledge for the future of the drier environments. ICARDA.

Robinson, D. A., Campbell, C. S., Hopmans, J. W., Hornbuckle, B. K., Jones, S. B., Knight, R., Ogden, F., Selker, J., and Wendroth, O. (2008). Soil moisture measurement for ecological and hydrological watershed-scale observatories: A review. Vadose Zone Journal, 7(1), 358-389. https://doi.org/10.2136/vzj2007.0143

Samouëlian A., Cousin I., Tabbagh A., Bruand A., & Richard G. (2005). Electrical resistivity survey in soil science: A review. Soil and Tillage Research, 83(2), 173–193. https://doi.org/10.1016/j.still.2004.10.004

Savicka, M., & Škute, N. (2010). Effects of high temperature on malondialdehyde content, superoxide production and growth changes in wheat seedlings (Triticum aestivum L.). Ekologija, 56(1), 26–33. https://doi.org/10.2478/v10055-010-0004-x

Saxton, K.E. 2005. Soil water characteristics hydraulic properties calculator. http://hydrolab.arsusda.gov/soilwater/Index.htm.

Şen Z. (2008). Wadi hydrology. CRC Press.

Seutra Kaba, J., Abunyewa, A. A., Kugbe, J., Kwashie, G. K. S., Owusu Ansah, E., & Andoh, H. (2021). Arbuscular mycorrhizal fungi and potassium fertilizer as plant biostimulants and alternative research for enhancing plants adaptation to drought stress: Opportunities for enhancing drought tolerance in cocoa (Theobroma cacao L.). Sustainable Environment, 7(1). https://doi.org/10.1080/27658511.2021.1963927

Sharma, P., Jha, A. B., Dubey, R. S., & Pessarakli, M. (2012). Reactive Oxygen Species, Oxidative Damage, and Antioxidative Defense Mechanism in Plants under Stressful Conditions. Journal of Botany, 2012, 1–26. https://doi.org/10.1155/2012/217037

Steelman C.M., & Endres A.L. (2011). Comparison of petrophysical relationships for soil moisture estimation using GPR ground waves. Vadose Zone Journal, 10(1), 270–285. https://doi.org/10.2136/vzj2010.0040

Stoffregen H., Zenker T., & Wessolek G. (2002). Accuracy of soil water content measurements using ground penetrating radar: Comparison of ground penetrating radar and lysimeter data. Journal of Hydrology, 267(3–4), 201–206. https://doi.org/10.1016/S0022-1694(02)00150-6

Taamallah, H. 2003. Carte pédologique de la Jeffara. Rapport interne, projet Jeffara, IRA/IRD, Tunis.

Tahyaoui. H (2007) : Nappe des grès du Trias de sahel el ababsa de Médenine : Aspects hydrogéologiques et Proposition d'une gestion durable. Rapport interne. DGRE

Tejera García, N. A., Olivera, M., Iribarne, C., & Lluch, C. (2004). Partial purification and characterization of a non-specific acid phosphatase in leaves and root nodules of Phaseolus vulgaris. Plant Physiology and Biochemistry, 42(7–8), 585–591. https://doi.org/10.1016/j.plaphy.2004.04.004

Topp G.C., Davis J.L., & Annan A.P. (1980). Electromagnetic determination of soil water content: Measurements in coaxial transmission lines. Water Resources Research, 16(3), 574–582. https://doi.org/10.1029/WR016i003p00574

Toubali, S., Tahiri, A. I., Anli, M., Symanczik, S., Boutasknit, A., Ait-El-mokhtar, M., Ben-Laouane, R., Oufdou, K., Ait-Rahou, Y., Ben-Ahmed, H., Jemo, M., Hafidi, M., & Meddich, A. (2020). Physiological and biochemical behaviors of date palm vitroplants treated with microbial consortia and compost in response to salt stress. Applied Sciences (Switzerland), 10(23), 1–25. https://doi.org/10.3390/app10238665

Tosti F., & Slob E. (2015). Determination, by using GPR, of the volumetric water content in structures, substructures, foundations and soil. In Civil engineering applications of ground penetrating radar (pp. 163–189). Springer International Publishing. https://doi.org/10.1007/978-3-319-04813-0_8

USDA Soil Conservation Service. 1983. National Engineering Handbook Section 4 Hydrology, Chapter 19.

Velikova, V., Yordanov, I., & Edreva, A. (2000). Oxidative stress and some antioxidant systems in acid rain-treated bean plants: Protective role of exogenous polyamines. Plant Science, 151(1), 59–66. https://doi.org/https://doi.org/10.1016/S0168-9452(99)00197-1

Waxman, M. H., and Smits, L. J. M. (1968). Electrical conductivities in oil-bearing shaly sands. Society of Petroleum Engineers Journal, 8(2), 107-122.

Wahid, F., Fahad, S., Danish, S., Adnan, M., Yue, Z., Saud, S., Siddiqui, M. H., Brtnicky, M., Hammerschmiedt, T., & Datta, R. (2020). Sustainable management with mycorrhizae and phosphate solubilizing bacteria for enhanced phosphorus uptake in calcareous soils. Agriculture (Switzerland), 10(8), 1–14. https://doi.org/10.3390/agriculture10080334

Weiler K.W., Steenhuis T.S., Boll J., & Kung K.-J.S. (1998). Comparison of ground penetrating radar and time-domain reflectometry as soil water sensors. Soil Science Society of America Journal, 62(5), 1237–1239. https://doi.org/10.2136/sssaj1998.03615995006200050013x

Wheater H.S. (2002). Hydrological processes in arid and semi-arid areas. In H.S. Wheater & R.A. Al-Weshah (Eds.), Hydrology of wadi systems (pp. 5–22). UNESCO, IHP-V, Technical Documents in Hydrology No. 55.

Wollschläger U., & Roth K. (2005). Estimation of temporal changes of volumetric soil water content from ground-penetrating radar reflections. Subsurface Sensing Technologies and Applications, 6(2), 207–218. https://doi.org/10.1007/s11220-005-0007-y

Yahyaoui H. & M. Ouessar 2000. Abstraction and recharge impacts on the ground water in the arid regions of Tunisia: Case of Zeuss-Koutine water table. Proceedings of the international workshop on Water management in dry areas, Médenine, Tunisia; 18-22 October 1999, UNU Desertification Series N°2, 72-78.

Yahyaoui, H., Chaieb, H., Ouessar, M. 2002. Impact des travaux de conservation des eaux et des sols sur la recharge de la nappe de Zeuss-Koutine (Médenine: Sud-est tunisien).

Yahyaoui. H (1996). Etude hydrogéologique des aquifères du Piémont Oriental et du flanc Occidental du Dahar (Régions de Remada et de Déhibat). Thèse Doct, Fac. Sc. De Tunis, 171 p.

Yahyaoui H (2001) Nappe des Grès du Trias du Sahel El Ababssa. Aspects hydrogéologiques et mobilisation des ressources. DGRE, Tunis

Ye, Q., Wang, H., & Li, H. (2022). Arbuscular Mycorrhizal Fungi Improve Growth, Photosynthetic Activity, and Chlorophyll Fluorescence of Vitis vinifera L. cv. Ecolly under Drought Stress. Agronomy, 12(7). https://doi.org/10.3390/agronomy12071563

Zaouchi, Y., Rezgui, S., & Bettaieb, T. (2015). Influence of mycorrhization on adaptation capacity of Jacaranda mimosifolia D . Don grown in urban conditions. Journal of New Sciences, 18(5), 679–688.

Zarei, A. R. (2018). Evaluation of Drought Condition in Arid and Semi- Arid Regions, Using RDI Index. Water Resources Management, 32(5), 1689–1711. https://doi.org/10.1007/s11269-017-1898-9

Zhu, X. C., Song, F. B., Liu, S. Q., Liu, T. D., & Zhou, X. (2012). Arbuscular mycorrhizae improves photosynthesis and water status of Zea mays L. under drought stress. Plant, Soil and Environment, 58(4), 186–191. https://doi.org/10.17221/23/2011-pse